

# Mathematical modelling of the first HIV/ZIKV co-infection cases in Colombia and Brazil

Jhoana P. Romero-Leiton · Idriss Sekkak · Julien Arino · Bouchra Nasri

Received: date / Accepted: date

**Abstract** This paper presents a mathematical model to investigate co-infection with HIV/AIDS and zika virus (ZIKV) in Colombia and Brazil, where the first cases were reported in 2015-2016. The model considers the sexual transmission dynamics of both viruses and vector-host interactions. We begin by exploring the qualitative behaviour of each model separately. Then, we analyze the dynamics of the co-infection model using the thresholds and results defined separately for each model. The model also considers the impact of intervention strategies, such as, personal protection, antiretroviral therapy (ART), and sexual protection (condoms use). Using available parameter values for Colombia and Brazil, the model is calibrated to predict the potential effect of implementing combinations of those intervention strategies on the co-infection spread. According to these findings, transmission through sexual contact is a determining factor in the long-term behaviour of these two diseases. Furthermore, it is important to note that co-infection with HIV and ZIKV may result in higher rates of HIV transmission and an increased risk of severe congenital disabilities linked to ZIKV infection. As a result, control measures have been implemented to limit the number of infected individuals and mosquitoes, with the aim of halting disease transmission. This study provides novel insights into the dynamics of HIV/ZIKV co-infection and highlights the importance of integrated intervention strategies in controlling the spread of these viruses, which may impact public health.

**Keywords** Stability · Equilibrium points · Optimal control · Personal protection · Sexual protection · Antiretroviral therapy · Model calibration.

## 1 Introduction

Human immunodeficiency virus (HIV) and zika virus (ZIKV) are two major public health concerns worldwide, particularly in Latin America and Caribbean countries [1]. While HIV is a chronic infection that attacks the immune system, ZIKV is transmitted by mosquitoes and can even cause congenital malformations, such as Guillain-Barré syndrome [2-4] and microcephaly [5, 6]. On the one hand, if HIV is not treated, it can cause Acquired Immunodeficiency Syndrome (AIDS). This virus can be transmitted through sexual contact, syringe misuse, and vertically (from mother to child) [7]. HIV/AIDS still has no cure, so treatments seek to lower or reduce the level of virus replication in the body of infected people, which consists of a mixture of different drugs, commonly called antiretroviral (or combined) therapy (ART) [8]. On the other hand, ZIKV,

---

J. P. Romero-Leiton & Julien Arino  
Department of Mathematics, University of Manitoba,  
Winnipeg MB R3T 1E9 Canada.  
E-mail: jhoana.romero@umanitoba.ca & julien.arino@umanitoba.ca

I. Sekkak & B. Nasri  
Département de Médecine Sociale et Préventive,  
École de Santé Publique de l'Université de Montréal, Montreal QC H3N 1X9 Canada.  
E-mail: idriss.sekkak@umontreal.ca & bouchra.nasri@umontreal.ca

unlike other arboviruses, also presents transmission through sexual contact. Some studies have demonstrated its detection and transmission through semen, urine, and saliva [9–11].

Thus, although HIV is not a zoonotic disease, it shares specific transmission characteristics with ZIKV. Both viruses can be transmitted through sexual contact and vertically from mother to fetus. These additional modes of transmission can significantly increase the risk of other sexually transmitted infections in endemic regions, particularly HIV, for both the mother and the fetus [12]. There are few case reports of ZIKV infection in HIV-infected individuals [13]. The first recorded case of HIV/ZIKV co-infection was confirmed in a 38-year-old patient in a Rio de Janeiro (Brazil) laboratory in 2016 [6]. In the same region, a zika case was reported in an HIV-infected pregnant woman [14, 15]. The fetus exhibited significant abnormalities, consistent with research on pregnant women in Brazil who were infected with ZIKV [16], and the fetus ultimately died. In 2018, five individuals from the departments of Risaralda and Sucre were informed of HIV/ZIKV co-infection in Colombia [1]. Fortunately, these patients had reasonable immune and virologic controls when infected with ZIKV, with no relevant differences from patients infected with ZIKV alone.

However, additional research is necessary to understand better the interactions between HIV/ZIKV co-infection and their impact on immune response, disease severity, and control [1]. The question remains unanswered as to whether HIV infection increases the likelihood of contracting ZIKV and whether ZIKV infection could worsen HIV infection, particularly during pregnancy. Nevertheless, laboratory studies have revealed that placental tissues are vulnerable to ZIKV infection [12]. In addition to causing placental dysfunction in co-infections, ZIKV infection significantly affects the host's immune response. A recent study indicated that ZIKV primarily targets CD14+ monocytes, particularly during pregnancy, resulting in inflammatory reactions and immune tolerance [12]. However, ZIKV has the potential to facilitate HIV infection by promoting HIV replication through the release of cytokines that can activate CD4+ T cells or by binding directly to HIV proteins that encourage HIV replication. Unlike HIV, the relationship between mother-to-child transmission of ZIKV and fetal disease caused by ZIKV infection has not yet been established. However, even in the presence of ART, acute viral infection is likely to intensify immune system dysfunction in HIV-infected pregnant women, increasing the risk and consequences of mother-to-child transmission of HIV and ZIKV [17]. Therefore, the potential interaction between HIV and ZIKV has recently garnered significant attention. These interactions can modify the epidemiology, pathogenesis, immune response, and therapy of both infections. For instance, co-infection can expedite HIV pathogenesis and enhance transmission by boosting viral replication efficiency. Additionally, the spread of ZIKV infection may reveal new and more severe clinical manifestations in immunocompromised individuals exposed to the virus.

Given the potential impact of HIV/ZIKV co-infection on public health, it is crucial to understand the transmission dynamics of these viruses and evaluate the effectiveness of intervention strategies. Mathematical models are crucial for understanding and providing valuable insights into public health policy decisions. To our knowledge, there is no evidence of mathematical models studying this phenomenon in the literature. Therefore, this study aimed to formulate and analyze an HIV/ZIKV co-infection model, assuming that both diseases are sexually transmitted, and ZIKV is also mosquito-transmitted. The analysis of this model is expected to identify important transmission factors that will help design and evaluate different control and prevention strategies to minimize their impact on public health.

The organization of this study is as follows: In Section 2, the co-infection model is introduced, providing a comprehensive understanding of its structure and dynamics. Subsequently, Sections 2.1 and 2.2 present the individual dynamics of the HIV-only and ZIKV-only models, respectively, highlighting the unique characteristics of each infection. Section 3 focuses on the analysis of the co-infection model, delving into the interplay and synergistic effects between HIV and ZIKV. The optimal control problem is addressed analytically in Section 4, emphasizing the exploration of strategies to mitigate the spread and impact of the co-infection. Furthermore, in Section 5, a case study centred in Colombia and Brazil is presented, whereby the uncontrolled and controlled models are numerically analyzed using data derived from the comprehensive literature review. Finally, in Section 6, a discussion and concluding remarks are provided, encompassing the modelling approach, its results, along with prospects for future research and unresolved questions.

## 2 The HIV/ZIKV mathematical model formulation

This model examines two distinct groups: the human (host) and mosquito (vector) populations. We assumed that an individual who is susceptible to either disease cannot be infected with both diseases simultaneously at the same time. The total number  $N(t)$  of people in the human population at a given time is divided into six categories: those who are susceptible to both viruses, denoted as  $S(t)$ ; those who are infected with only ZIKV but still susceptible to HIV, denoted as  $I_z(t)$ ; those who are infected with only HIV but still susceptible to ZIKV, denoted as  $I_h(t)$ ; those who are infected with both HIV and ZIKV simultaneously, denoted as  $I_{hz}(t)$ ; those who are infected with AIDS, denoted as  $A(t)$ ; and those who have recovered from ZIKV, denoted as  $R(t)$ . Thus, the total human population can be represented as the sum of all these categories ( $N(t) = S(t) + I_z(t) + I_h(t) + I_{hz}(t) + A(t) + R(t)$ ), as shown in Tables 2.1-2.2.

The total mosquito population  $N_m(t)$  at time  $t$  can be classified into two compartments: the susceptible mosquito population  $S_m(t)$  and the ZIKV-carrying mosquitoes  $I_m(t)$ . Thus,  $N_m(t) = S_m(t) + I_m(t)$  (see Tables 2.1 and 2.2).

Variable	Description
$N(t)$	The total human population at time $t$
$S(t)$	Susceptible human population at time $t$
$I_z(t)$	Infected human population with only ZIKV at time $t$
$I_h(t)$	Infected human population with only HIV at time $t$
$I_{hz}(t)$	Infected human population with ZIK/HIV at time $t$
$A(t)$	Infected human population with AIDS at time $t$
$R(t)$	Recovered human population of ZIKV at time $t$
$N_m(t)$	The total mosquito population at time $t$
$S_m(t)$	Susceptible mosquito population at time $t$
$I_m(t)$	ZIKV-carrying mosquito population at time $t$

Table 2.1: Description of the state variables involved in Model (2.1).

Parameter	Description	Dimension
$\Lambda$	Recruitment rate of humans	$pop \times time^{-1}$
$\beta_m$	Infection rate of humans by contact with infected mosquitoes with ZIKV	$(pop \times time)^{-1}$
$\beta_z$	Infection rate of humans by contact with humans infected with ZIKV through sexual contact	$(pop \times time)^{-1}$
$\beta_h$	Infection rate of humans by contact with humans infected with HIV through sexual contact	$(pop \times time)^{-1}$
$1/\sigma_1$	Mean duration of the immunodeficiency period	time
$1/\sigma_2$	Mean duration of the immunodeficiency period in co-infected individuals	time <sup>-1</sup>
$1/\mu$	Human mean lifespan	time
$\mu_z$	Mortality rate by zika	time <sup>-1</sup>
$\mu_h$	Mortality rate by AIDS	time <sup>-1</sup>
$\mu_{hz}$	Mortality rate by ZIKV/AIDS	time <sup>-1</sup>
$1/\delta_z$	Mean duration of the zika infection	time
$\omega_1$	Transition probability from zika to HIV/ZIKV co-infection	Dimensionless
$\omega_2$	Transition probability from HIV to HIV/ZIKV co-infection	Dimensionless
$\epsilon$	Modification parameter or decrease recovery rate factor	Dimensionless
$\Lambda_m$	Recruitment rate of mosquitoes	$pop \times time^{-1}$
$\alpha_m$	Infection rate of mosquitoes by contact with infected humans with ZIKV	$(pop \times time)^{-1}$
$1/\mu_m$	Mosquito mean lifespan	time

Table 2.2: Description and dimension of the parameters involved in Model (2.1).

$$\left\{ \begin{array}{l}
 \frac{dS}{dt} = \Lambda - (\beta_m I_m + \beta_z I_z + \beta_h I_h) S - \mu S \\
 \frac{dI_z}{dt} = (\beta_m I_m + \beta_z I_z) S - \omega_2 \beta_h I_z I_h - (\mu_z + \delta_z + \mu) I_z \\
 \frac{dI_h}{dt} = \beta_h I_h S - \omega_1 (\beta_m I_m + \beta_z I_z) I_h - (\sigma_1 + \mu) I_h \\
 \frac{dI_{hz}}{dt} = \omega_1 (\beta_m I_m + \beta_z I_z) I_h + \omega_2 \beta_h I_h I_z - \epsilon \delta_z I_{hz} - (\sigma_2 + \mu_{hz} + \mu) I_{hz} \\
 \frac{dA}{dt} = \sigma_1 I_h + \sigma_2 I_{hz} - (\mu_h + \mu) A \\
 \frac{dR}{dt} = \delta_z I_z + \epsilon \delta_z I_{hz} - \mu R \\
 \frac{dS_m}{dt} = \Lambda_m - \alpha_m (I_z + I_{hz}) S_m - \mu_m S_m \\
 \frac{dI_m}{dt} = \alpha_m (I_z + I_{hz}) S_m - \mu_m I_m
 \end{array} \right. \quad (2.1)$$

Figure 2.1 illustrates the dynamics depicted by the equations involved in Model (2.1)..

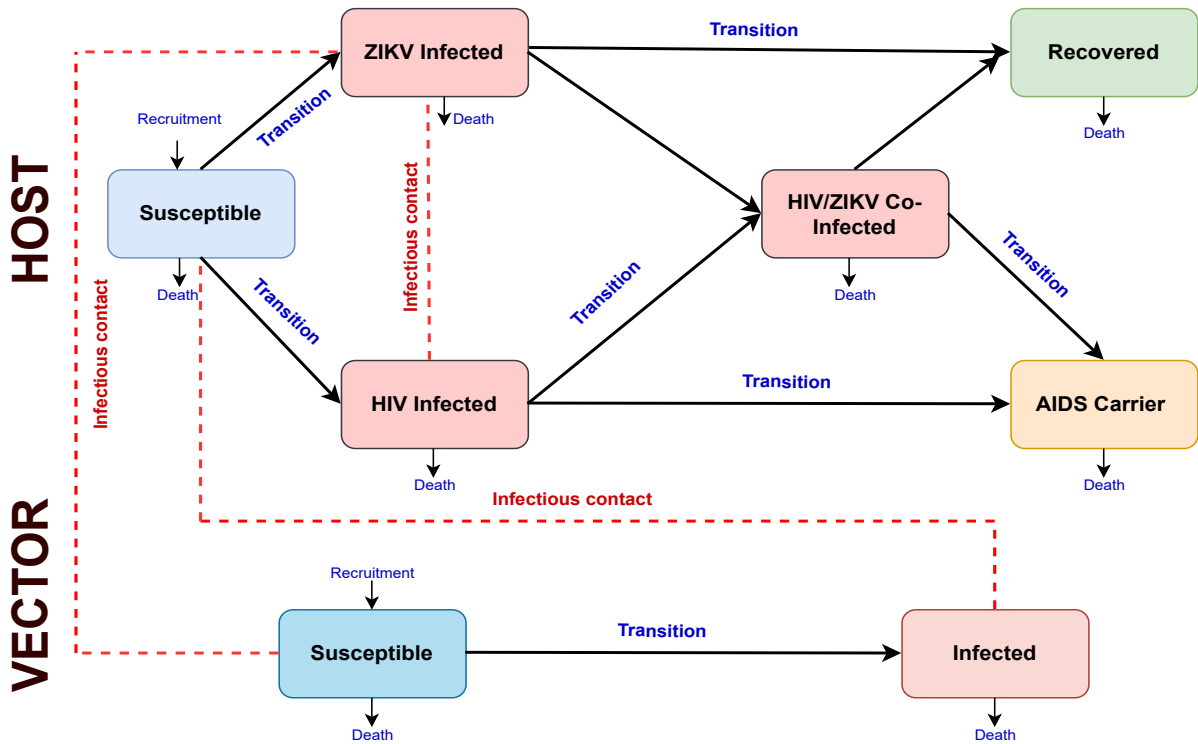


Fig. 2.1: HIV/ZIKV co-infection model represented in Model (2.1).

In the following two sections, we qualitatively analyse the properties of System (2.1). We will start by analysing the dynamics of the two component models: the HIV/AIDS model and the ZIKV model.

## 2.1 Qualitative behaviour of the HIV/AIDS model

The HIV/AIDS model, is obtained by setting  $I_z = I_{hz} = R = S_m = I_m = 0$  in System (2.1). Thus, the ODEs described in (2.1) can be rewritten as:

$$\begin{cases} \frac{dS}{dt} = \Lambda - \beta_h I_h S - \mu S \\ \frac{dI_h}{dt} = \beta_h I_h S - (\sigma_1 + \mu) I_h \\ \frac{dA}{dt} = \sigma_1 I_h - (\mu_h + \mu) A, \end{cases} \quad (2.2)$$

where the total human population is  $N_h(t) = S(t) + I_h(t) + A(t)$ . For this model, the region of biological interest is

$$\Omega_h = \left\{ (S, I_h, A) \in \mathbb{R}_+^3 : 0 \leq N_h \leq \frac{\Lambda}{\mu} \right\}. \quad (2.3)$$

It can be proved that  $\Omega_h$  is positively-invariant under the flow of (2.2) (see e.g., [18]), that is, all solutions of System (2.2) starting in  $\Omega_h$  remain in  $\Omega_h$  for all  $t \geq 0$ . Therefore, it is enough to consider the dynamics of (2.2) in  $\Omega_h$ .

The disease-free equilibrium (DFE) of Model (2.2) is given by

$$\mathbf{E}_{h_0} = \left( \frac{\Lambda}{\mu}, 0, 0 \right), \quad (2.4)$$

which is obtained when  $I_h = A = 0$ . The stability of this equilibrium point can be analyzed in terms of the basic reproduction number for the HIV/AIDS model ( $\mathcal{R}_h$ ), which can be computed using the next-generation operator [19]. Using the notation of [18] in Model (2.2) the matrices  $\mathbf{F}$  and  $\mathbf{V}$  are given by

$$\mathbf{F} = \begin{bmatrix} \beta_h \frac{\Lambda}{\mu} & 0 \\ 0 & 0 \end{bmatrix}, \quad \text{and} \quad \mathbf{V} = \begin{bmatrix} \sigma_1 + \mu & 0 \\ -\sigma_1 & \mu_h + \mu \end{bmatrix}.$$

Therefore, it follows that  $\mathcal{R}_h$  associated to Model (2.2) is given by

$$\mathcal{R}_h = \rho(\mathbf{F}\mathbf{V}^{-1}) = \frac{\beta_h}{\sigma_1 + \mu} \frac{\Lambda}{\mu}, \quad (2.5)$$

where  $\rho$  represents the spectral radius of the matrix  $\mathbf{F}\mathbf{V}^{-1}$ .

To determine the endemic equilibrium points of Model(2.2), we must solve the system of algebraic equations

$$\begin{cases} 0 = \Lambda - \beta_h I_h S - \mu S \\ 0 = \beta_h I_h S - (\sigma_1 + \mu) I_h \\ 0 = \sigma_1 I_h - (\mu_h + \mu) A. \end{cases} \quad (2.6)$$

After some algebraic manipulations for  $I_h, A \neq 0$ , we find that the solutions of System (2.6) are

$$S^* = \frac{\sigma_1 + \mu}{\beta_h}, \quad I_h^* = \frac{\mu}{\beta_h} (\mathcal{R}_h - 1) \quad \text{and} \quad A^* = \frac{\mu \sigma_1}{\beta_h (\mu_h + \mu)} (\mathcal{R}_h - 1).$$

Thus, as long as  $\mathcal{R}_h > 1$ , System (2.2) has an endemic equilibrium point given by

$$\mathbf{E}_h^* = \left( \frac{\sigma_1 + \mu}{\beta_h}, \frac{\mu}{\beta_h}(\mathcal{R}_h - 1), \frac{\mu\sigma_1}{\beta_h(\mu_h + \mu)}(\mathcal{R}_h - 1) \right). \quad (2.7)$$

The local stability of  $\mathbf{E}_{h_0}$  defined on (2.4) and  $\mathbf{E}_h^*$  defined on (2.7) is determined by the sign of the eigenvalues of the linearisation matrix (Jacobian matrix) of System (2.2) around them. The Jacobian matrix of System (2.2) at an arbitrary point  $\mathbf{E} = (S, I_h, A)$  is

$$\mathbf{J}(\mathbf{E}) = \begin{bmatrix} -(\beta_h I_h + \mu) & -\beta_h S & 0 \\ \beta_h I_h & \beta_h S - (\sigma_1 + \mu) & 0 \\ 0 & \sigma_1 & -(\mu_h + \mu) \end{bmatrix} = \begin{bmatrix} \mathbf{J}_{11}(\mathbf{E}) & \mathbf{0} \\ \star & -(\mu_h + \mu) \end{bmatrix}, \quad (2.8)$$

so eigenvalues of  $\mathbf{J}(\mathbf{E})$  are  $-(\mu_h + \mu) < 0$  and those of  $\mathbf{J}_{11}(\mathbf{E})$ . At  $\mathbf{E}_{h_0}$ ,

$$\mathbf{J}_{11}(\mathbf{E}_{h_0}) = \begin{bmatrix} -\mu & -\beta_h \frac{\Lambda}{\mu} \\ 0 & (\sigma_1 + \mu)(\mathcal{R}_h - 1) \end{bmatrix}$$

is upper triangular with eigenvalues  $-\mu < 0$  and  $(\sigma_1 + \mu)(\mathcal{R}_h - 1)$ . At  $\mathbf{E}_h^*$ ,

$$\mathbf{J}_{11}(\mathbf{E}_h^*) = \begin{bmatrix} -\mu\mathcal{R}_h - (\sigma_1 + \mu) & \\ \mu\mathcal{R}_h & 0 \end{bmatrix}.$$

Thus  $\mathbf{J}_{11}(\mathbf{E}_h^*)$  has positive determinant and negative trace, implying eigenvalues with negative real parts when  $\mathbf{E}_h^*$  is biologically relevant, i.e., when  $\mathcal{R}_h > 1$ . These results are summarized in the following proposition.

**Proposition 1** *System (2.2) always has a DFE  $\mathbf{E}_{h_0}$  given in (2.4), and for  $\mathcal{R}_h > 1$  defined in (2.5), also exists an endemic equilibrium point  $\mathbf{E}_h^*$  given in (2.7). Additionally, if  $\mathcal{R}_h < 1$  the DFE is locally asymptotically stable (LAS) in  $\Omega_h$  defined in (2.3), whereas  $\mathbf{E}_h^*$  is unstable. If  $\mathcal{R}_h > 1$ , then  $\mathbf{E}_h^*$  is LAS in  $\Omega_h$  and the DFE becomes an unstable hyperbolic point.*

As it is well known, the basic reproduction number of an infection  $\mathcal{R}_h$  is the average number of new cases generated by a given case throughout an infectious period. Thus, Proposition 1 tells us that HIV infection can be controlled in the community if the initial values of the subpopulation of the model are in the region of attraction of  $\mathbf{E}_{h_0}$ . Therefore, to ensure that the control of the virus is independent of initial conditions, we must prove the global asymptotic stability (GAS) of the equilibrium points. We obtain the following result.

**Proposition 2** *If  $\mathcal{R}_h < 1$ , the DFE  $\mathbf{E}_{h_0}$  of Model (2.2), is GAS. If  $\mathcal{R}_h > 1$ , the endemic equilibrium point  $\mathbf{E}_h^*$ , is GAS.*

The proof of global asymptotic stability of the DFE when  $\mathcal{R}_h < 1$  is found in Appendix A.1. The global asymptotic stability of  $\mathbf{E}_h^*$  when  $\mathcal{R}_h > 1$  is found in Appendix A.2.

## 2.2 Qualitative behaviour of the ZIKV model

By setting  $I_h = I_{hz} = A = 0$  in System (2.1), we obtain the ZIKV model as follows

$$\begin{cases} \frac{dS}{dt} = \Lambda - (\beta_m I_m + \beta_z I_z) S - \mu S \\ \frac{dI_z}{dt} = (\beta_m I_m + \beta_z I_z) S - (\mu_z + \delta_z + \mu) I_z \\ \frac{dR}{dt} = \delta_z I_z - \mu R \\ \frac{dS_m}{dt} = \Lambda_m - \alpha_m I_z S_m - \mu_m S_m \\ \frac{dI_m}{dt} = \alpha_m I_z S_m - \mu_m I_m \end{cases} \quad (2.9)$$

For this model, the total human population is  $N_z(t) = S(t) + I_z(t) + R(t)$ , and the total mosquito population is  $N_m(t) = S_m(t) + I_m(t)$ . We are interested in analyzing the solutions within the biological region of interest

$$\Omega_z = \left\{ (S, I_z, R, S_m, I_m) \in \mathbb{R}_+^5 : 0 \leq N_h \leq \frac{\Lambda}{\mu}; 0 \leq N_m \leq \frac{\Lambda_m}{\mu_m} \right\}. \quad (2.10)$$

It can also be shown that  $\Omega_z$  is positively invariant under the flow of (2.9).

The DFE for Model (2.9) is given by

$$\mathbf{E}_{z_0} = \left( \frac{\Lambda}{\mu}, 0, 0, \frac{\Lambda_m}{\mu_m}, 0 \right). \quad (2.11)$$

Now, we will determine the basic reproduction number  $\mathcal{R}_z$  for Model (2.9). Similarly as in Section 2.1, the matrices  $\mathbf{F}$  and  $\mathbf{V}$  are given by

$$\mathbf{F} = \begin{bmatrix} \beta_z \frac{\Lambda}{\mu} & \beta_m \frac{\Lambda}{\mu} \\ \alpha_m \frac{\Lambda_m}{\mu_m} & 0 \end{bmatrix}, \quad \text{and} \quad \mathbf{V} = \begin{bmatrix} \delta_z + \mu + \mu_z & 0 \\ 0 & \mu_m \end{bmatrix}.$$

Thus, the basic reproduction number for Model (2.9) is given by

$$\mathcal{R}_z = \rho(\mathbf{F}\mathbf{V}^{-1}) = \mathcal{R}_{z_1} + \sqrt{(\mathcal{R}_{z_1})^2 + \bar{\mathcal{R}}_{z_2}} =: \mathcal{R}_{z_1} + \mathcal{R}_{z_2}, \quad (2.12)$$

where

$$\mathcal{R}_{z_1} = \frac{\beta_z \Lambda}{2\mu(\mu_z + \delta_z + \mu)}, \quad \bar{\mathcal{R}}_{z_2} = \frac{\beta_m \alpha_m \Lambda_m \Lambda}{\mu \mu_m^2 (\mu_z + \delta_z + \mu)} \quad \text{and} \quad \mathcal{R}_{z_2} = \sqrt{(\mathcal{R}_{z_1})^2 + \bar{\mathcal{R}}_{z_2}}. \quad (2.13)$$

*Remark 1* Note that if the transmission of ZIKV by sexual contact is not considered ( $\beta_z = 0$ ),  $\mathcal{R}_{z_1} = 0$  and  $\mathcal{R}_z$  reduces to

$$\mathcal{R}_z|_{(\beta_z=0)} = \sqrt{\bar{\mathcal{R}}_{z_2}} = \sqrt{\frac{\beta_m \alpha_m \Lambda_m \Lambda}{\mu \mu_m^2 (\mu_z + \delta_z + \mu)}},$$

indicating that sexual contact transmission of ZIKV has an impact on  $\mathcal{R}_z$ .

The following lemma makes it easier to determine the sign of  $\mathcal{R}_z$ .

**Lemma 1** *Let us define*

$$\begin{aligned} \mathcal{R}_z^* &= 2\mathcal{R}_{z_1} + \bar{\mathcal{R}}_{z_2} \\ &=: \mathcal{R}_z^2 + 2\mathcal{R}_{z_1}(1 - \mathcal{R}_z). \end{aligned} \quad (2.14)$$

- i. If  $\mathcal{R}_z^* < 1$ , then  $2\mathcal{R}_{z_1} < 1$  and  $\mathcal{R}_z < 1$ .
- ii. If  $\mathcal{R}_z^* > 1$  and  $2\mathcal{R}_{z_1} < 1$ , then  $\mathcal{R}_z > 1$ .
- iii. If  $\mathcal{R}_z^* > 1$  and  $2\mathcal{R}_{z_1} > 1$ , then  $\mathcal{R}_z < 1$ .
- iv. If  $\mathcal{R}_z^* = 1$ , then  $\mathcal{R}_z = 1$ .

The proof can be found in Appendix A.3.

From the above lemma we can see that the sign of  $\mathcal{R}_z$  is determined by the signs of  $\mathcal{R}_z^*$  and  $2\mathcal{R}_{z_1}$ .

We can now determine the local asymptotic stability of the DFE  $\mathbf{E}_{z_0}$ . To this end, we order equations and variables as  $S, S_m, I_z, I_m, R$  and compute the Jacobian matrix of System (2.9) at an arbitrary point  $\mathbf{E} = (S, S_m, I_z, I_m, R)$ , which is given by

$$\mathbf{J}(\mathbf{E}) = \begin{bmatrix} \mathbf{J}_{11}(\mathbf{E}) & \mathbf{0} \\ \star & -\mu \end{bmatrix}. \quad (2.15)$$

Thus, the eigenvalues of  $\mathbf{J}(\mathbf{E})$  are  $-\mu < 0$  and those of  $\mathbf{J}_{11}(\mathbf{E})$ . At  $\mathbf{E}_{z_0}$

$$\mathbf{J}_{11}(\mathbf{E}_{z_0}) = \begin{bmatrix} -\mu & 0 & -\beta_z \Lambda / \mu & -\beta_m \Lambda / \mu \\ 0 & -\mu_m & -\alpha_m \Lambda_m / \mu_m & 0 \\ 0 & 0 & \beta_z \Lambda / \mu - (\mu_z + \delta_z + \mu) & \beta_m \Lambda_m / \mu_m \\ 0 & 0 & \alpha_m \Lambda_m \mu_m & -\mu_m \end{bmatrix} = \begin{bmatrix} \mathbf{D}_{11} & \star \\ 0 & \mathbf{D}_{22} \end{bmatrix}.$$

Again, the above matrix is  $2 \times 2$  block upper triangular with (1,1) block being a diagonal matrix with diagonal entries (eigenvalues)  $-\mu < 0$  and  $-\mu_m < 0$ . So all that remains to determine the eigenvalues of the  $2 \times 2$  matrix

$$\mathbf{D}_{22} = \begin{bmatrix} \beta_z \frac{\Lambda}{\mu} - (\mu_z + \delta_z + \mu) \beta_m \frac{\Lambda_m}{\mu_m} & \\ & \alpha_m \frac{\Lambda_m}{\mu_m} & -\mu_m \end{bmatrix}.$$

After some algebraic manipulations, we found that the above matrix has associated the following characteristic polynomial.

$$q(x) = x^2 + a_1x + a_2, \quad \text{where} \quad (2.16)$$

$$a_1 = \mu_m - (\mu_z + \delta_z + \mu)(2\mathcal{R}_{z_1} - 1)$$

$$a_2 = \mu_m(\mu_z + \delta_z + \mu)(1 - R_z^*).$$

Note that all roots of the characteristic polynomial  $q(x)$  have a negative real part if  $\mathcal{R}_z^*$  defined in (2.14) satisfies  $\mathcal{R}_z^* < 1$  (see Lemma 1). We have the following result.

**Proposition 3** *If  $\mathcal{R}_z^* < 1$ , then  $\mathbf{E}_{z_0}$  defined in (2.11) is LAS in  $\Omega_z$  defined in (2.10).*

Now, in order to determine the endemic equilibrium points of System (2.9), we have to solve the following system of algebraic equations

$$\begin{cases} 0 = \Lambda - (\beta_m I_m + \beta_z I_z) S - \mu S \\ 0 = (\beta_m I_m + \beta_z I_z) S - (\mu_z + \delta_z + \mu) I_z \\ 0 = \delta_z I_z - \mu R \\ 0 = \Lambda_m - \alpha_m I_z S_m - \mu_m S_m \\ 0 = \alpha_m I_z S_m - \mu_m I_m. \end{cases} \quad (2.17)$$

To this end, we first define the following threshold

$$R_{max} = \frac{\Lambda}{\mu} \frac{\delta_z}{\mu_z + \delta_z + \mu}. \quad (2.18)$$

Therefore, after some algebraic manipulations in (2.17), we can write the variables  $S$ ,  $I_z$ ,  $S_m$  and  $I_m$  in terms of the variable  $R$  and the thresholds defined in (2.18) as follows.

$$\begin{aligned} S &= \frac{\Lambda}{\mu} \left( 1 - \frac{R}{R_{max}} \right), & I_z &= \frac{\mu}{\delta_z} R, \\ S_m &= \frac{\Lambda_m}{\mu_m} \left( 1 - \frac{\alpha_m \mu R}{\mu_m \delta_z + \alpha_m \mu R} \right), & I_m &= \frac{\alpha_m \Lambda_m \mu}{\mu_m \delta_z + \alpha_m \mu R} R. \end{aligned} \quad (2.19)$$

From the above expressions, it can be observed that  $S_m$  is always positive (because  $\mu_m \delta_z + \alpha_m \mu R > \alpha_m \mu R$  and, if  $R < R_{max}$  then  $S > 0$ ). Replacing the above values into the second equation of (2.17), we get the following quadratic equations in the variable  $R$ :

$$aR^2 + bR + c = 0, \quad \text{where} \quad (2.20)$$

$$\begin{aligned}
a &= \frac{\beta_z \Lambda \alpha_m \mu}{\delta_z R_{max}} \\
b &= \frac{\mu(\mu_z + \delta_z + \mu)}{\delta_z} \left[ \frac{\beta_m \alpha_m \Lambda_m}{\mu_m} + \beta_z \mu_m + \alpha_m \mu (1 - 2\mathcal{R}_{z_1}) \right] \\
c &= (\mu_z + \delta_z + \mu) \mu \mu_m (1 - \mathcal{R}_z^*).
\end{aligned} \tag{2.21}$$

Note that  $a > 0$ , and the signs of  $b$  and  $c$  depends on the sign of  $\mathcal{R}_z^*$  and  $2\mathcal{R}_{z_1}$ . We have the following possibilities.

- P1) If  $\mathcal{R}_z^* < 1$ , then  $2\mathcal{R}_{z_1} < 1$  (Lemma 2.14 item *i*). Therefore  $b > 0$  y  $c > 0$  and thus, the quadratic equation (2.20) has not any positive root.
- P2) If  $\mathcal{R}_z^* > 1$ , then  $c < 0$  and regardless of the sign of  $b$ , the quadratic equation (2.20) has only one positive root given by

$$R^* = \frac{-b + \sqrt{b^2 - 4ac}}{2a}. \tag{2.22}$$

- P3) If  $\mathcal{R}_z^* = 1$  and  $2\mathcal{R}_{z_1} < 1$ , then  $c = 0$  and  $b > 0$ . Therefore, the quadratic equation (2.20) has as solution  $R = -b/a$ . Thus, there are no positive roots.
- P4) If  $\mathcal{R}_z^* = 1$  and  $b < 0$ , the quadratic equation (2.20) has a positive root given by  $R = -b/a$ .

*Remark 2* The case  $\mathcal{R}_z^* < 1$  and  $2\mathcal{R}_{z_1} > 1$  ( $c > 0$  and  $b < 0$ ), which gives the possibility of the existence of two positive roots for the quadratic equation (2.20) whenever  $b^2 - 4ac > 0$ , is not considered since by Lemma 2.14 item *i*, when  $\mathcal{R}_z^* < 1$  leads to  $2\mathcal{R}_{z_1} < 1$ .

Based on the information presented earlier, the quadratic equation (2.20) has only one positive root defined in (2.22) whenever  $\mathcal{R}_z^* > 1$ . The proof that the condition  $R^* < R_{max}$  is satisfied can be found in Appendix A.4. Thus, we can ensure the conditions for the existence of the endemic equilibrium point.

**Proposition 4** *If  $\mathcal{R}_z^* > 1$  System (2.9) has an endemic equilibrium point given by*

$$\mathbf{E}_z^* = \left( \frac{\Lambda}{\mu} \left( 1 - \frac{R^*}{R_{max}} \right), \frac{\mu}{\delta_z} R^*, R^*, \frac{\Lambda_m}{\mu_m} \left( 1 - \frac{\alpha_m \mu R^*}{\mu_m \delta_z + \alpha_m \mu R^*} \right), \frac{\alpha_m \Lambda_m \mu}{\mu_m \delta_z + \alpha_m \mu R^*} R^* \right), \tag{2.23}$$

with  $R_{max}$  given in (2.18) and  $R^*$  in (2.22).

We have already stated in Proposition 3 the local asymptotic stability of the DFE. In a similar way, we can prove the local asymptotic stability of the endemic equilibrium  $\mathbf{E}_z^*$ . To this end, we determine the sign of the eigenvalues of the matrix defined in (2.15) evaluated in  $\mathbf{E}_z^*$ . In order to simplify algebraic manipulations we make the following change of variables

$$\begin{aligned}
\kappa &= \mu_z + \delta_z + \mu, \quad t_1 = \beta_m I_m^* + \beta_z I_z^*, \\
t_2 &= \beta_z S^*, \quad t_3 = \beta_m S^*, \\
t_4 &= \alpha_m S_m^*, \quad t_5 = \alpha_m I_z^*,
\end{aligned}$$

thus, the matrix  $\mathbf{J}(\mathbf{E}_z^*)$  can be rewritten as

$$\mathbf{J}(\mathbf{E}_z^*) = \begin{bmatrix} -(t_1 + \mu) & -t_2 & 0 & 0 & -t_3 \\ t_1 & t_2 - \kappa & 0 & 0 & t_3 \\ 0 & \delta_z & -\mu & 0 & 0 \\ 0 & -t_4 & 0 & -(t_5 + \mu_m) & 0 \\ 0 & t_4 & 0 & t_5 & -\mu_m \end{bmatrix}.$$

After some algebraic manipulations, we find that the characteristic polynomial associated to the matrix  $\mathbf{J}(\mathbf{E}_z^*)$  is

$$r(y) = (y + \mu)(y + \mu_m)(y^3 + b_1y^2 + b_2y + b_3), \quad \text{where} \quad (2.24)$$

$$b_1 = t_6 + \kappa(1 - 2\mathcal{R}_{z_1})$$

$$b_2 = t_7 + \kappa(\mathcal{R}_z^* - 1)$$

$$b_3 = t_8(\mathcal{R}_z^* - 1),$$

and  $t_6$ ,  $t_7$  and  $t_8$  defined as a positive linear combination of  $t_i$ ,  $i = 1, \dots, 5$ . The characteristic polynomial  $r(y)$  gives five roots, two of them are  $y = -\mu$  and  $y = -\mu_m$ , whereas the Routh-Hurtwitz criteria assures that the other three roots have negative real part if  $b_i > 0$  for  $i = 1, 2, 3$  and  $b_1b_2 - b_3 > 0$ . Clearly the coefficients  $b_i > 0$ ,  $i = 1, 2, 3$  are all positive if  $\mathcal{R}_z^* > 1$  and  $1 - 2\mathcal{R}_{z_1} > 0$ . Thus, it follows that the endemic equilibrium  $\mathbf{E}_z^*$  of System (2.9) is LAS if  $\mathcal{R}_z^* > 1$ . To conclude the qualitative analysis of Model (2.9), we prove the global stability of the DFE ( $\mathbf{E}_{z_0}$ ) using similar techniques to those used in Section 2.1.

**Proposition 5** *If  $\mathcal{R}_z^* > 1$ , the endemic equilibrium point  $\mathbf{E}_z^*$  defined in (2.23), is LAS in  $\Omega_z$  defined in (2.10). Conversely, if  $\mathcal{R}_z^* < 1$ , the DFE  $\mathbf{E}_{z_0}$  of Model (2.2) defined in (2.11), is GAS.*

The proof of the global stability of  $\mathbf{E}_{z_0}$  when  $\mathcal{R}_z^* < 1$  can be found in Appendix A.5.

### 3 Qualitative behaviour of the HIV/ZIKV model

In this section, we discuss the qualitative properties of the HIV/ZIKV co-infection model (2.1). To achieve this purpose, we use the existence and stability results as well as the definition of the basic reproduction number for the HIV model  $\mathcal{R}_h$  in (2.5) and  $\mathcal{R}_z$  in (2.12) obtained in Sections 2.1 and 2.2.

In Model (2.1), the total human population is denoted by  $N(t) = N_h(t) + N_z(t)$ , and the total mosquito population is  $N_m(t) = S_m(t) + I_m(t)$ . Additionally, to simplify algebraic calculations we rename parameters:

$$\begin{aligned} \kappa_1 &= \mu_z + \delta_z + \mu, & \kappa_2 &= \sigma_1 + \mu, \\ \kappa_3 &= \sigma_2 + \mu_{hz} + \mu, & \kappa_4 &= \mu_h + \mu. \end{aligned} \quad (3.1)$$

The interest region set is given by

$$\Omega = \left\{ (S, I_z, I_h, I_{hz}, A, R, S_m, I_m) \in \mathbb{R}_+^8 : 0 \leq N \leq \frac{\Lambda}{\mu}; 0 \leq N_m \leq \frac{\Lambda_m}{\mu_m} \right\}. \quad (3.2)$$

As in the previous sections, it can be proved that  $\Omega$  is positively invariant under the flow of (2.1).

#### 3.1 Computation of the basic reproduction number

The DFE for Model (2.1) is given by

$$\mathbf{E}_0 = \left( \frac{\Lambda}{\mu}, 0, 0, 0, 0, 0, \frac{\Lambda_m}{\mu_m}, 0 \right). \quad (3.3)$$

Similarly to Sections 2.1 and 2.2, the basic reproduction number associated to Model (2.1) can be determined through the matrices  $\mathbf{F}$  and  $\mathbf{V}$  given by

$$\mathbf{F} = \begin{bmatrix} \beta_z \frac{\Lambda}{\mu} & 0 & 0 & 0 & \beta_m \frac{\Lambda}{\mu} \\ 0 & \beta_m \frac{\Lambda}{\mu} & 0 & 0 & 0 \\ 0 & 0 & 0 & 0 & 0 \\ 0 & \sigma_1 & \sigma_2 & 0 & 0 \\ \alpha_m \frac{\Lambda_m}{\mu_m} & 0 & \alpha_m \frac{\Lambda_m}{\mu_m} & 0 & 0 \end{bmatrix}, \quad \text{and} \quad \mathbf{V} = \begin{bmatrix} \kappa_1 & 0 & 0 & 0 & 0 \\ 0 & \kappa_2 & 0 & 0 & 0 \\ 0 & 0 & \epsilon\delta_z + \kappa_3 & 0 & 0 \\ 0 & 0 & 0 & \kappa_4 & 0 \\ 0 & 0 & 0 & 0 & \mu_m \end{bmatrix}.$$

Here, the matrix  $\mathbf{FV}^{-1}$  is given by

$$\mathbf{FV}^{-1} = \begin{bmatrix} \beta_z \frac{\Lambda}{\mu\kappa_1} & 0 & 0 & 0 & \beta_m \frac{\Lambda}{\mu\mu_m} \\ 0 & \beta_m \frac{\Lambda}{\mu\kappa_2} & 0 & 0 & 0 \\ 0 & 0 & 0 & 0 & 0 \\ 0 & \frac{\sigma_1}{\kappa_2} & \frac{\sigma_2}{\epsilon\delta_z + \kappa_3} & 0 & 0 \\ \alpha_m \frac{\Lambda_m}{\mu_m \kappa_1} & 0 & \alpha_m \frac{\Lambda_m}{\mu_m (\epsilon\delta_z + \kappa_3)} & 0 & 0 \end{bmatrix}.$$

The above matrix has as eigenvalues  $\lambda_{1,2} = 0$  (twice) and  $\lambda_3 = \frac{\beta_h \Lambda}{\mu\kappa_2} = \mathcal{R}_h$ , whereas the other two eigenvalues are

$$\lambda_{4,5} = \frac{\beta_z \Lambda}{2\mu\kappa_1} \pm \sqrt{\left(\frac{\beta_z \Lambda}{2\mu\kappa_1}\right)^2 + \frac{\alpha_m \beta_m \Lambda_m \Lambda}{\mu\mu_m^2 \kappa_1}} = \mathcal{R}_{z_1} \pm \mathcal{R}_{z_2},$$

with the positive eigenvalues being

$$\lambda_4 = \frac{\beta_z \Lambda}{2\mu\kappa_1} + \sqrt{\left(\frac{\beta_z \Lambda}{2\mu\kappa_1}\right)^2 + \frac{\alpha_m \beta_m \Lambda_m \Lambda}{\mu\mu_m^2 \kappa_1}} = \mathcal{R}_{z_1} + \mathcal{R}_{z_2} = \mathcal{R}_z.$$

Thus, the basic reproduction number for Model (2.1) is given by

$$\mathcal{R}_0 = \rho(\mathbf{FV}^{-1}) = \max\{\mathcal{R}_h, \mathcal{R}_z\}, \quad (3.4)$$

where  $\mathcal{R}_h$  is the basic reproduction number for the HIV model defined in the equation (2.5) and  $\mathcal{R}_z = \mathcal{R}_{z_1} + \mathcal{R}_{z_2}$  is the basic reproduction number of the ZIKV model, which is defined in the equation (2.12).

### 3.2 Local sensitivity analysis of the parameters

A local sensitivity analysis of  $\mathcal{R}_0$  with respect to model parameters allows quantifying parameter variations' effect on the value of  $\mathcal{R}_0$ . The sign of the sensitivity index denotes the direction of the change, where a positive index for a particular parameter indicates that increasing that parameter will increase  $\mathcal{R}_0$  and vice versa. In addition, the magnitude of the sensitivity index provides insight into the relative significance of each parameter in the model predictions [20].

The normalized sensitivity index of a variable concerning a parameter is a measure of how much the variable relatively changes to the change in the parameter [21]. In other words, the normalized sensitivity index of the variable  $X$ , which is differentially dependent on parameter  $p$ , is defined as:

$$\Gamma_p^X = \frac{\partial X}{\partial p} \frac{p}{X}. \quad (3.5)$$

Because  $\mathcal{R}_0$  is defined as  $\max\{\mathcal{R}_h, \mathcal{R}_z\}$ , the sensitivity indices of  $\mathcal{R}_0$  with respect to the eleven parameters  $\{\beta_h, \Lambda, \mu, \sigma_1, \beta_z, \mu_z, \delta_z, \beta_m, \alpha_m, \Lambda_m, \mu_m\}$  in the expression of  $\mathcal{R}_0$  in (3.4), can be determined for the sensitivity indices of  $\mathcal{R}_h$  and  $\mathcal{R}_z$ , respectively. A calculation example of the sensitivity index of  $\mathcal{R}_z$  with respect to the parameter  $\beta_z$  can be found in Appendix A.6.

### 3.3 Stability analysis

Similarly to in Sections 2.1 and 2.2, the local stability of the DFE  $\mathbf{E}_0$  is determined by the linearization of (2.1) around an arbitrary equilibrium. By ordering the equations and variables as  $S, S_m, I_z, I_m, I_h, I_{hz}, A, R$  and computing the Jacobian matrix of System (2.9) at an arbitrary equilibrium point  $\mathbf{E} = (S, S_m, I_z, I_m, I_h, I_{hz}, A, R)$ , we obtain

$$\mathbf{J}(\mathbf{E}) = \begin{bmatrix} \mathbf{J}_{11}(\mathbf{E}) & \mathbf{0} & \mathbf{0} \\ \mathbf{0} & -\kappa_4 & \mathbf{0} \\ \mathbf{0} & \mathbf{0} & -\mu \end{bmatrix}. \quad (3.6)$$

The matrix shown above has eigenvalues  $-\mu < 0$ ,  $-\kappa_4 = -(\mu_h + \mu) < 0$  and the eigenvalues of  $\mathbf{J}_{11}(\mathbf{E})$ . By evaluating the matrix  $\mathbf{J}_{11}$  at the DFE  $\mathbf{E}_0$  we obtain

$$\mathbf{J}_{11}(\mathbf{E}_0) = \begin{bmatrix} -\mu & \mathbf{0} & \star & \star \\ \mathbf{0} & -\mu_m & \star & \star \\ \mathbf{0} & \mathbf{0} & \mathbf{M}_{33} & \star \\ \mathbf{0} & \mathbf{0} & \mathbf{0} & \mathbf{D}_{44} \end{bmatrix}, \text{ where } \mathbf{M}_{33} = \begin{bmatrix} -\kappa_1 + \frac{\Lambda\beta_z}{\mu} & \frac{\Lambda\beta_m}{\mu} \\ \frac{\Lambda_m\alpha_m}{\mu_m} & -\mu_m \end{bmatrix}$$

and  $\mathbf{D}_{44}$  is a diagonal matrix with entries  $-(\epsilon\delta_z + \kappa_3) < 0$  and  $\kappa_2 - \frac{\beta_h\Lambda}{\mu} = \sigma_1 + \mu - \frac{\beta_h\Lambda}{\mu} = (\sigma_1 + \mu)(1 - \mathcal{R}_h) < 0$  if and only if  $\mathcal{R}_h < 1$ . Therefore, the remaining eigenvalues of  $\mathbf{J}_{11}(\mathbf{E}_0)$  are those of the matrix  $\mathbf{M}_{33}$ , whose characteristic equation is

$$\lambda^2 + c_1\lambda + c_2 = 0, \quad (3.7)$$

where

$$c_1 = \kappa_1 + \mu_m - \frac{\beta_z\Lambda}{\mu} = \mu_m + \kappa_1(1 - 2\mathcal{R}_{z_1})$$

$$c_2 = \kappa_1\mu_m - \frac{\alpha_m\beta_m\Lambda_m\Lambda}{\mu\mu_m} - \frac{\beta_z\Lambda\mu_m}{\mu} = k_1\mu_m(1 - \mathcal{R}_z^*).$$

Thus, the roots of the equation (3.7) have negative real part if and only if  $\mathcal{R}_z^* < 1$  and  $2\mathcal{R}_{z_1} < 1$ , where  $\mathcal{R}_z^*$  and  $\mathcal{R}_{z_1}$  are defined in (2.14) and (2.13), respectively. We have the following result:

**Proposition 6** *If  $\mathcal{R}_0 = \max\{\mathcal{R}_h, \mathcal{R}_z\} < 1$ , then  $\mathbf{E}_0$  defined in (3.3) is LAS in  $\Omega$  defined in (3.2).*

Techniques similar to those used in Sections 2.1 and 2.2 can be applied to confirm the presence of endemic solutions and assess their local and global stability.

#### 4 The control problem analysis

In this section, we formulate an optimal control problem (OCP) by adding three intervention strategies to control the spread of HIV/ZIKV co-infection to Model (2.1). The proposed approach mitigates HIV and zika infections through the implementation of personal protection measures (such as the use of repellents) using control  $\eta_1$ , the use of ART with control  $\eta_2$  and preventive sexual contact (such as condom use) with control  $\eta_3$ . The control functions  $\eta_1$ ,  $\eta_2$  and  $\eta_3$  are defined in the interval  $[0, T]$ , where  $T$  denotes the final time of the controls,  $0 \leq \eta_i(t) \leq 1$  and  $t \in [0, T]$  for  $i = 1, 2, 3$ . Based on the aforementioned considerations, the following OCP is formulated, where the controls are shown in red for emphasis.

$$\left\{ \begin{array}{l}
\min \mathcal{J}(\eta) = \int_0^T \left( c_1 I_z + c_2 I_h + c_3 I_{hz} + c_4 I_m + c_5 A + d_1 \frac{\eta_1^2}{2} + d_2 \frac{\eta_2^2}{2} + d_3 \frac{\eta_3^2}{2} \right) dt \\
\frac{dS}{dt} = \Lambda - [(1 - \eta_1)\beta_m I_m + (1 - \eta_3)(\beta_z I_z + \beta_h I_h)] S - \mu S \\
\frac{dI_z}{dt} = [(1 - \eta_1)\beta_m I_m + (1 - \eta_3)\beta_z I_z] S - \omega_2 (1 - \eta_3)\beta_h I_z I_h - (\mu_z + \delta_z + \mu) I_z \\
\frac{dI_h}{dt} = (1 - \eta_3)\beta_h I_h S - \omega_1 [(1 - \eta_1)\beta_m I_m + (1 - \eta_3)\beta_z I_z] I_h - [(1 - \eta_2)\sigma_1 + \mu] I_h \\
\frac{dI_{hz}}{dt} = \omega_1 [(1 - \eta_1)\beta_m I_m + (1 - \eta_3)\beta_z I_z] I_h + \omega_2 (1 - \eta_3)\beta_h I_h I_z - \epsilon \delta_z I_{hz} - [(1 - \eta_2)\sigma_2 + \mu_{hz} + \mu] I_{hz} \\
\frac{dA}{dt} = (1 - \eta_2)\sigma_1 I_h + (1 - \eta_2)\sigma_2 I_{hz} - (\mu_h + \mu) A \\
\frac{dR}{dt} = \delta_z I_z + \epsilon \delta_z I_{hz} - \mu R \\
\frac{dS_m}{dt} = \Lambda_m - (1 - \eta_1)\alpha_m (I_z + I_{hz}) S_m - \mu_m S_m \\
\frac{dI_m}{dt} = (1 - \eta_1)\alpha_m (I_z + I_{hz}) S_m - \mu_m I_m \\
\mathbf{X}(0) = (S_0, I_{z0}, I_{h0}, I_{hz0}, A_0, R_0, S_{m0}, I_{m0}) = \mathbf{X}_0 \\
\mathbf{X}(T) = (S_f, I_{zf}, I_{hf}, I_{hzf}, A_f, R_f, S_{mf}, I_{mf}) = \mathbf{X}_f.
\end{array} \right. \quad (4.1)$$

In the above formulation  $\eta = (\eta_1(t), \eta_2(t), \eta_3(t))$ , and  $c_1, c_2, c_3, c_4, c_5, d_1, d_2$ , and  $d_3$  are positive weights. Therefore, we seek an optimal control  $\eta^*(t)$  determined as

$$\mathcal{J}(\eta^*(t)) = \min \{ \mathcal{J}(\eta(t) | \eta \in \mathcal{A}) \}, \quad (4.2)$$

with a set  $\mathcal{A}$  of controls defined as

$$\mathcal{A} = \{ \eta(t) = (\eta_1(t), \eta_2(t), \eta_3(t)) | 0 \leq \eta_1(t) \leq \eta_1^{\max}, 0 \leq \eta_2(t) \leq \eta_2^{\max}, 0 \leq \eta_3(t) \leq \eta_3^{\max} \},$$

where  $\eta_i^{\max} \leq 1$ ,  $i = \{1, 2, 3\}$  and  $\eta$  is Lebesgue measurable. In order to define the formulation of our OCP using Pontryagin's Maximum Principle (PMP) [22], we have the Lagrangian as

$$L = c_1 I_z(t) + c_2 I_h(t) + c_3 I_{hz}(t) + c_4 I_m(t) + c_5 A(t) + d_1 \frac{\eta_1^2(t)}{2} + d_2 \frac{\eta_2^2(t)}{2} + d_3 \frac{\eta_3^2(t)}{2}, \quad (4.3)$$

and we determine the Hamiltonian function as

$$H = L(I_z, I_h, I_{hz}, I_m, A, \eta) + p_1 \frac{dS}{dt} + p_2 \frac{dI_z}{dt} + p_3 \frac{dI_h}{dt} + p_4 \frac{dI_{hz}}{dt} + p_5 \frac{dA}{dt} + p_6 \frac{dR}{dt} + p_7 \frac{dS_m}{dt} + p_8 \frac{dI_m}{dt}. \quad (4.4)$$

In the remainder, we investigate the minimum value of Lagrangian (4.3). Firstly, we must prove existence of the optimal control  $\eta^*$  according to the controlled system (4.1).

**Proposition 7** *There exists an optimal control  $\eta^*$  such that*

$$\mathcal{J}(\eta^*(t)) = \min_{\eta \in \mathcal{A}} (\mathcal{J}(\eta(t))),$$

*subject to Control System (4.1) with initial conditions as  $\mathbf{X}_0$ .*

The proof of the above proposition can be found in Appendix A.7.

In the following, we apply PMP [22] to provide a characterization of an optimal control solution to the Hamiltonian (4.4) subject to the OCP (4.1). If  $(X^*, \eta^*)$  is an optimal solution for the controlled system (4.1), then there exists a non trivial vector function  $p = (p_1, p_2, p_3, p_4, p_5, p_6, p_7, p_8)$ , such that

$$\frac{\partial H}{\partial \eta_i} = 0, \quad i = 1, 2, 3 \quad \text{and} \quad \dot{p}_i = \frac{dp_i}{dt} = -\frac{\partial H}{\partial X_i}, \quad i = 1, \dots, 8. \quad (4.5)$$

**Proposition 8** *Let  $(S^*, I_z^*, I_h^*, I_{hz}^*, A^*, R^*, S_m^*, I_m^*)$  be the optimal state variables solution associated to the optimal control variable  $\eta^*$  subject to the control problem (4.2). Then, there exists an adjoint vector  $p$  that satisfies the controlled system (4.1), with transversality conditions  $p_i(T) = 0$ , for  $i = 1, \dots, 8$ , where the optimal controls are*

$$\begin{aligned} \eta_1^* &= \frac{((p_2 - p_1)S + (p_4 - p_3)I_h) \beta_m I_m + (p_8 - p_7)\alpha_m(I_z + I_{hz})S_m}{d_1} \\ \eta_2^* &= \frac{(p_5 - p_3) \sigma_1 I_h + (p_5 - p_4) \sigma_2 I_{hz}}{d_2} \\ \eta_3^* &= \frac{(p_2 - p_1)\beta_z I_z S + (p_3 - p_1)\beta_h I_h S + (p_4 - p_3)\omega_1 \beta_z I_z I_h + (p_4 - p_2)\omega_2 \beta_h I_z I_h}{d_3}. \end{aligned} \quad (4.6)$$

The proof is in Appendix A.8.

## 5 HIV/ZIKV co-infection in Brazil and Colombia

As mentioned previously, during 2015 and 2016, Brazil and Colombia experienced an alarming occurrence involving the co-infection of two significant viral diseases: HIV/AIDS and zika. This phenomenon emerged as a complex public health issue challenging the healthcare system in these regions. In fact, the co-infection highlighted the need for further research, comprehensive surveillance, and implementation of prevention and early reaction strategies to mitigate the impact of these dual infections.

Owing to the lack of temporal records on HIV/ZIKV co-infection to date, it was not possible to estimate the parameters of Model (2.1) in this section. However, specific parameter values were derived from available demographic information and previous research conducted on zika and HIV/AIDS in Colombia and Brazil. In cases where there was a lack of available data, these values were either estimated based on specific assumptions or adapted from research conducted on different regions or diseases. The following outlines the main assumptions for extracting these parameter values.

Firstly, the precise relationship between humans and population densities of *Aedes aegypti* remains uncertain and has been a subject of considerable interest and investigation within the field of entomology. Examining the existing literature, it can be inferred that during 2015-2016, there existed an approximate ratio of one human to three female *Aedes aegypti* mosquitoes (1:3) in Colombia and Brazil. Secondly, the modification parameter related to the recovery rate of humans  $\epsilon$  was assumed to be much smaller than one because, according to research in this area, an individual with HIV/ZIKV co-infection recovers more slowly than an individual with only zika [12, 13, 17, 23, 24]. Thirdly, the parameters associated with the co-infection probability  $w_1$  and  $w_2$  were assumed to be small because by 2016, only five cases had been reported in Colombia and one in Brazil [1, 6]. However, a hypothetical scenario in which these parameters are escalated is depicted to demonstrate the correlation between rising probabilities of co-infection and the subsequent increase in the number of co-infected individuals. Finally, certain parameter values pertaining to HIV/AIDS were predominantly adjusted at a population level, drawing upon estimations derived from Luxembourg, the Czech Republic, Japan, Croatia, the United Kingdom, and Mexico [25].

As in [26], we assume that Colombia and Brazil share some common parameter values (see Table 5.1), except for those related to country population size and initial conditions (see Table 5.2).

Due to the dispersion of the units of measurement of the parameters in the different sources consulted, all parameter values were adapted to *day* as the unit of measurement.

Parameter	Range	Reference
$\delta_z$	[1.11e-2, 7.14e-2]	[26]
$\sigma_1$	[2.1e-4, 5.46e-4]	[25]
$\mu_h$	5.46e-5	[25]
$\mu_m$	[5e-2, 1.2e-1]	[26]
$\mu_z$	[3.42e-5, 5.46e-5]	Assumed
$\mu_{hz}$	0	[1, 6]
$\sigma_2$	4.55e-5	[1, 6]
$\omega_1$	[1e-3, 1e-2]	[1, 6]
$\omega_2$	[1e-3, 1e-2]	[1, 6]
$\epsilon$	1e-10	[1, 6]

Table 5.1: Shared (Colombia-Brazil) range of parameter values (minimum and maximum) involved in Model (2.1). Time in days.

Parameter	Colombia	Brazil	Reference
$\beta_m$	[6.25e-10, 1.25e-9]	[2.42e-10, 2.9e-10]	[26]
$\beta_z$	[2.08e-12, 1.04e-11]	[4.83e-13, 2.42e-12]	[26]
$\beta_h$	[6.25e-12, 1.46e-11]	[1.45e-12, 3.38e-12]	[25]
$\alpha_m$	[2.08e-10, 4.17e-10]	[4.83e-11, 9.66e-11]	[26]
$\Lambda$	[1.73e+03, 1.73e+03]	[7.44e+03, 7.44e+03]	[27]
$\mu$	3.21e-5	3.21e-5	[27]
$\Lambda_m$	[1.03e+7, 1.03e+7]	[4.43e+7, 4.43e+7]	[27]

Table 5.2: Range of parameter values (minimum and maximum) involved in Model (2.1) that differ in Colombia and Brazil. Time in days.

Parameter	Colombia	Brazil	Reference
$S(0)$	28,800,000	124,200,000	[26]
$I_z(0)$	9,600,000	41,400,000	[26]
$I_h(0)$	4,320,000	18,630,000	[25]
$I_{hz}(0)$	4.8	20.7	[1, 6]
$A(0)$	2,832,000	12,213,000	[1, 6]
$R(0)$	2,448,000	10,557,000	[1, 6]
$S_m(0)$	33,600,000	144,900,000	[26]
$I_m(0)$	14,400,000	62,100,000	[26]

Table 5.3: Initial conditions involved in Model (2.1).

Once parameter values have been set, the case study is organized into three separate stages. The initial stage involves numerical determination of the basic reproduction number defined in Section 3.1. Furthermore, numerical values of the sensitivity indices determined analytically in Section 3.2 are also presented. In the second stage, the uncontrolled model defined by (2.1) is simulated numerically. Finally, the third stage focuses on numerically simulating the control problem described in (4.1). This sequential framework allows for a thorough exploration of the various aspects under investigation, providing a comprehensive analysis of the case study.

### 5.1 Value of the basic reproduction number and its sensitivity indices

In Section 3.1, we calculated the basic reproduction number (3.4) for Model (2.1). Figure 5.1 shows the possible values for the basic reproduction number using the extreme parameter values given in Tables 5.1 and 5.2 for Colombia and Brazil, that result in the minimum or maximum value of  $\mathcal{R}_0$ , respectively.

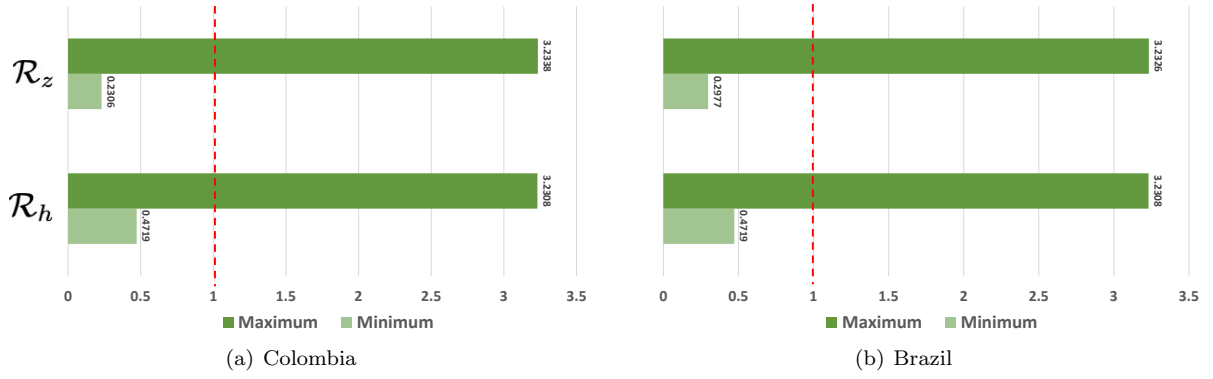


Fig. 5.1: Possible values for the thresholds using the extreme parameter values given in Tables 5.1 and 5.2 for Colombia and Brazil, that result in the minimum or maximum value of  $\mathcal{R}_0$ , respectively. In each case,  $\mathcal{R}_0 = \max\{\mathcal{R}_h, \mathcal{R}_z\}$ . The vertical red line represents  $\mathcal{R}_{h,z} = 1$ .

The normalized sensitivity indices of  $\mathcal{R}_h$  and  $\mathcal{R}_z$  summarized in Figure 5.2, are obtained using the values of the parameters in Tables 5.1 and 5.2.

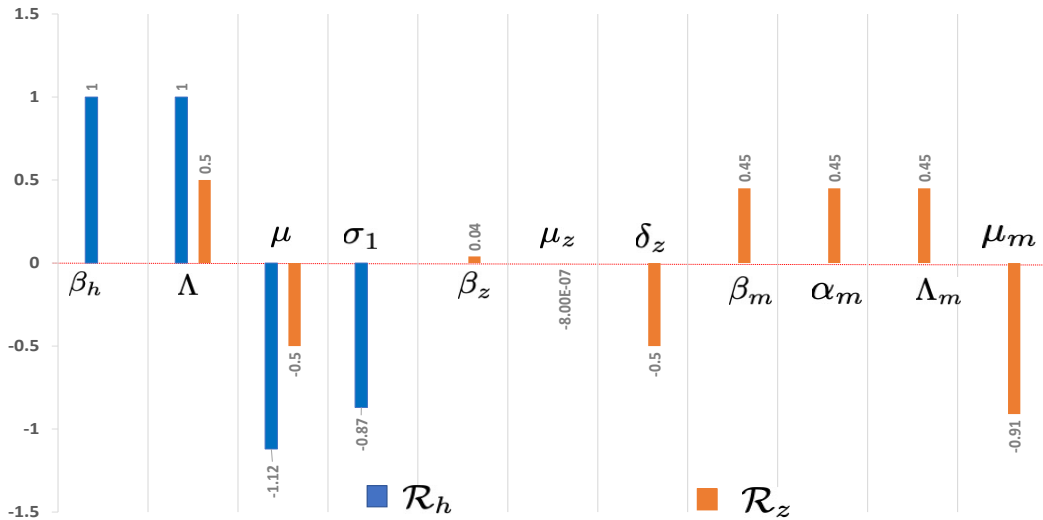


Fig. 5.2: Normalized sensitivity index of  $\mathcal{R}_h$  to the parameters  $\{\beta_h, \Lambda, \mu, \sigma_1\}$  and  $\mathcal{R}_z$  to the parameters  $\{\Lambda, \mu, \beta_z, \mu_z, \delta_z, \beta_m, \alpha_m, \Lambda_m, \mu_m\}$ . Thus, the red dot line represents sensitivity of zero. A calculation example using Equation (3.5) can be found in Appendix A.6.

Regarding  $\mathcal{R}_h$ , the primary driver is the human death rate  $\mu$ , followed by the infection rate  $\beta_h$  of humans through sexual contact with HIV-infected individuals and the human recruitment rate  $\Lambda$ . This implies that a reduction in the the human death rate  $\mu$  would result in the most significant increase in the likelihood of HIV infection among humans. Regarding  $\mathcal{R}_z$ , the outcomes reveal that the parameter with the highest impact is the mosquitoes death rate  $\mu_m$ : longer surviving mosquitoes lead to an increase in  $\mathcal{R}_z$ . Additionally, the human recruitment rate  $\Lambda$  and death rate  $\mu$  are also essential factors influencing  $\mathcal{R}_z$ .

## 5.2 Evaluation of uncontrolled population behaviour over time

We then performed numerical simulations of the uncontrolled Model (2.1). We begin by representing the DFE for Colombia and Brazil. The DFE is obtained when the value of  $\mathcal{R}_0$  is less than one. As shown in Figure 5.1, for Colombia and Brazil,  $\mathcal{R}_0=0.47192$ . Figure 5.3 shows the behaviour of the solutions for both human and mosquito populations. In both cases, on day 50 after the first observation, infected individuals (with either disease) tended to zero, whereas susceptible humans are stabilized. A similar scenario was observed in the mosquito population. On day 25 of the first observation, infected mosquitoes decreased to zero, and susceptible mosquitoes stabilized. In this scenario, HIV/AIDS cases outnumbered ZIKV cases. No outbreaks of infected individuals were observed under the initial conditions used. Similarly, the endemic equilibrium is obtained when the value of  $\mathcal{R}_0$  is greater than one (see Figure 5.1). This scenario is simulated and depicted in Figure 5.4. For Colombia  $\mathcal{R}_0=3.2338$  and for Brazil  $\mathcal{R}_0=3.2326$ . We can observe a significant increase in the number of individuals infected with ZIKV during the first 70 days of the first observation, with the number of HIV/AIDS-infected individuals being lower. Individuals infected with ZIKV reached maximum values on day 70 of the first observation. In contrast, individuals infected with HIV/AIDS did not generate peaks and appear to have a constant behaviour throughout the observed period (approximately a year). During the first 250 days from the first observation, ZIKV-infected individuals outnumber HIV/AIDS-infected individuals. However, after day 250, HIV/AIDS-infected individuals constantly outnumber ZIKV-infected individuals.

For the mosquito population, there is always a higher population density of susceptible than infected mosquitoes, but there is stable coexistence between them. Both countries differ mainly in population density (Brazil has a larger population than Colombia). The simulations indicated that the behaviour of both populations in Colombia and Brazil was highly similar, with a notable distinction in terms of population densities. This suggests that the dynamics and patterns of infection transmission were comparable between the two countries, with variations primarily related to the size of the populations being studied. An interesting observation from the simulations was that the behaviour of individuals infected with ZIKV displayed more significant variability than those infected with HIV/AIDS. This implies that the progression and manifestations of the ZIKV infection were more diverse and fluctuating, potentially influenced by various factors such as environmental conditions, viral load, or other epidemiological characteristics. In contrast, the behaviour of HIV/AIDS-infected individuals appeared to be more consistent and stable over time. These findings highlight the distinctive characteristics of ZIKV and HIV/AIDS infections, particularly in terms of the dynamic nature of zika infection compared to the relatively more constant nature of HIV/AIDS infection.

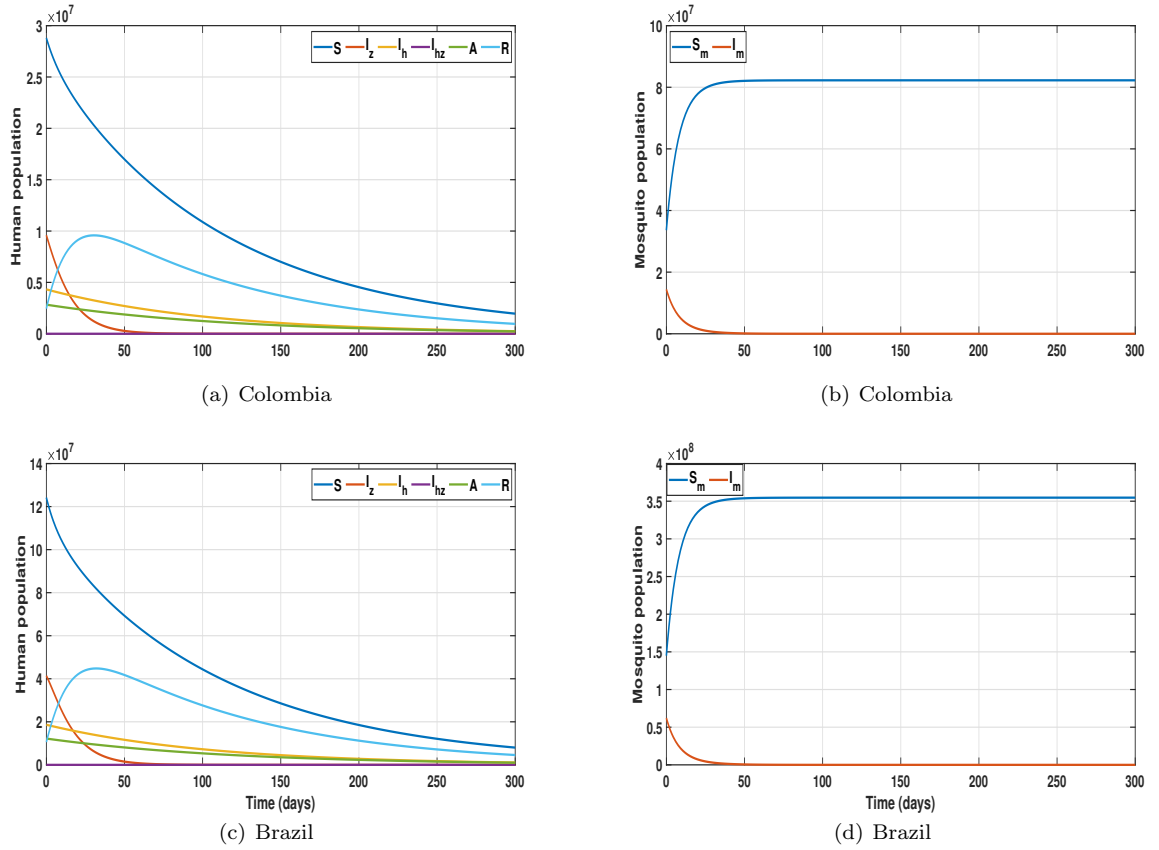


Fig. 5.3: Simulations of the DFE for Colombia and Brazil. For Colombia,  $\mathcal{R}_h = 0.4719$ ,  $\mathcal{R}_z = 0.2306$ . For Brazil,  $\mathcal{R}_h = 0.4719$ ,  $\mathcal{R}_z = 0.2977$ . In both countries,  $\mathcal{R}_0 = 0.4719$ . The solutions tend to the DFE.

A hypothetical scenario for HIV/ZIKV co-infected individuals is shown in Figure 5.5. We contrasted three different possibilities for the probability of co-infection:  $\omega_{1,2} = 0.001, 0.0055, 0.01$ . The first value (0.001) was named low probability, the second value (0.0055) medium probability and the last value (0.01) high probability. It can be seen that for higher values of this pair of parameters, a higher population density of individuals co-infected with ZIKV and HIV follows. Evidently, an increase in these two probabilities increased the density of co-infected individuals.

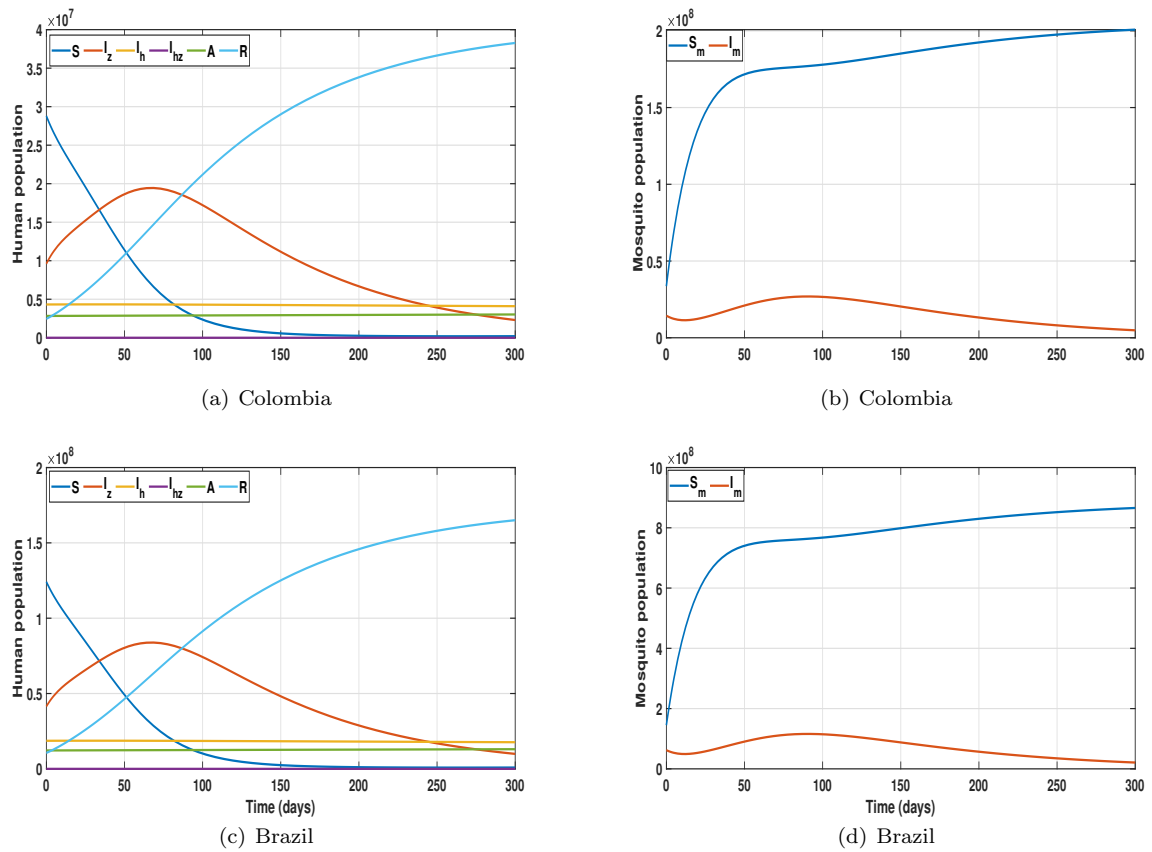


Fig. 5.4: Simulations of the endemic equilibrium. For Colombia,  $\mathcal{R}_h = 3.2308$ ,  $\mathcal{R}_z = 3.2338$ . For Brazil,  $\mathcal{R}_h = 3.2308$ ,  $\mathcal{R}_z = 3.2326$ . The solutions tend to the endemic equilibrium.

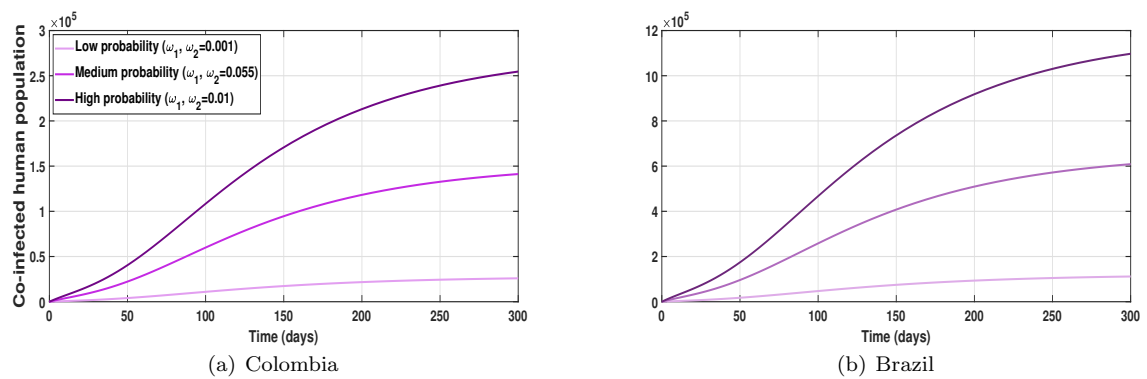


Fig. 5.5: HIV/ZIKV co-infected human population for different values of the co-infection probabilities  $\omega_1$  and  $\omega_2$ .

These numerical experiments showed that for values of  $\mathcal{R}_0 < 1$ , the HIV/ZIKV co-infection epidemics tend to fade away after some time, with infected individuals tending to zero and the susceptible population reaching a stable level. The same trend was observed for the mosquito population, with infected mosquitoes

decreasing to zero and susceptible mosquitoes stabilizing. A noticeable increase in the number of individuals infected with ZIKV, with a lower number of individuals infected with HIV/AIDS, was observed during the first 70 days of the first observation for the values of  $\mathcal{R}_0 > 1$ . Infected individuals with ZIKV peaked on day 70, whereas HIV-infected individuals did not generate any peaks during the 300 simulated days. Regarding the mosquito population, susceptible mosquitoes always outnumber infected mosquitoes; however, both coexist.

In addition, Figure 5.5 provides insights into the hypothetical scenario of ZIKV/HIV co-infection. Comparing three different scenarios for co-infection probabilities (high, medium and low), an increase in these probabilities above 0.01, leads to an increase in the density of co-infected individuals. These findings suggest that the values of these parameters can significantly impact the spread and severity of HIV/ZIKV co-infection, highlighting the importance of considering multiple factors when designing effective strategies to prevent and control the spread of these viruses, particularly in pregnant women to avoid congenital malformations in children.

These findings suggest that the behaviour of populations in Colombia and Brazil was similar but different in population densities. This suggests that the patterns of infection transmission were comparable, primarily influenced by population size. Notably, individuals infected with ZIKV exhibited more significant behaviour variability than those infected with HIV/AIDS. This indicates that ZIKV infection showed diverse and fluctuating progression and manifestations, potentially influenced by various factors. In contrast, HIV/AIDS-infected individuals displayed more consistent and stable behaviour over time.

### 5.3 Evaluation of controlled population behaviour over time

This stage focuses on numerically simulating the control problem described by (4.1). To this end, we investigate the effects of mixing strategies to control HIV/ZIKV co-infection in Colombia and Brazil. Table 5.4 shows the balancing and weighting constants values associated with the OPC (4.1).

Parameter	$c_1$	$c_1$	$c_3$	$c_4$	$d_1$	$d_2$	$d_3$
Value	0.5	0.5	0.5	0.5	$10^5$	$10^7$	$7 \times 10^6$

Table 5.4: Balancing and weighting constants values associated to the OPC (4.1).

On the one hand, controlling the spread of ZIKV and HIV in Colombia requires specialized actions to address the particular problems that the population has to overcome. To combat ZIKV, efforts must be directed toward preventing mosquito bites using insect repellents, protective clothing, and mosquito control measures. Therefore, the zika Fever Response Plan [28] enacted in 2016 was a priority for the Colombian government and focused on improving public health surveillance systems for vector-transmitted diseases and raising awareness of health issues [29]. To prevent sexually transmitted infections from spreading, safe sex practices must be emphasized in public health campaigns among vulnerable populations [30]. Therefore, ART and condoms are critical for controlling the spread of the human immunodeficiency virus. To ensure that people living with HIV in Colombia receive the care they require to be healthy and to lower their risk of spreading the virus to others, it is essential to increase access to HIV testing and treatment. Condom use and other harm reduction techniques must also be promoted in public health campaigns, especially among high-risk groups, such as drug injectors. By addressing these challenges through a comprehensive approach, including education, prevention, and access to care, Colombia can make significant progress in controlling the spread of ZIKV and HIV.

On the other hand, Brazil has implemented a countrywide strategy to manage *Aedes* mosquito populations and to stop the spread of ZIKV [31]. This effort has incorporated activities, including insecticide application, the elimination of standing water, and public awareness campaigns to motivate people to take action to lessen mosquito breeding grounds, which are incorporated as  $\eta_1$  in the epidemic model (4.1). Additionally, it has been noted that zika can be transmitted sexually; hence, condom use is advised as a preventative

measure. Brazil has implemented a comprehensive strategy for HIV prevention and care [32]. This has involved administering ART to all HIV-positive individuals since 2013. Brazil started a campaign to distribute condoms, encouraging condom use among vulnerable populations. As a result, the number of AIDS-related deaths in Brazil has significantly decreased.

Hence, using the controls  $\eta_1^*$ ,  $\eta_2^*$ , and  $\eta_3^*$  determined in Proposition 8 to optimize the controlled dynamical system (4.1), and by simulating the endemic scenario for Colombia and Brazil (Figure 5.4), we obtain in Figures 5.6–5.8 a timely controlled pattern. The sizes of humans infected with ZIKV, HIV/ZIKV, and HIV/AIDS are reduced due to mixed strategies to maintain the level of infection. However, the size of the HIV-infected population is increasing because of ART, resulting in better healthcare for the infected population, which helped to reduce the number of individuals with AIDS. In contrast, in Figure 5.6, ZIKV prevention measures helped reduce the number of infected mosquitoes and their contact with susceptible individuals.

In Figure 5.7, the control  $\eta_1$  is required at its full maximum at the beginning by establishing measures such as mosquito repellents and nets, elimination of mosquito breeding sites, and protective clothing.  $\eta_2$  goes in three months to its maximum capacity to contain the number of individuals who attended the AIDS stage, which slows the progression of the disease, prevents further damage to the immune system, and reduces the risk of HIV transmission. Additionally,  $\eta_3$  describes a gradual campaign to promote condom use can help reduce the transmission of HIV and increase awareness about the importance of protecting oneself and one's partners from sexually transmitted infections, such as educating people about the benefits of using condoms to prevent the spread of HIV, increasing easy access to condoms, and recruiting community leaders, influential individuals, or social media influencers to encourage the use of condoms.

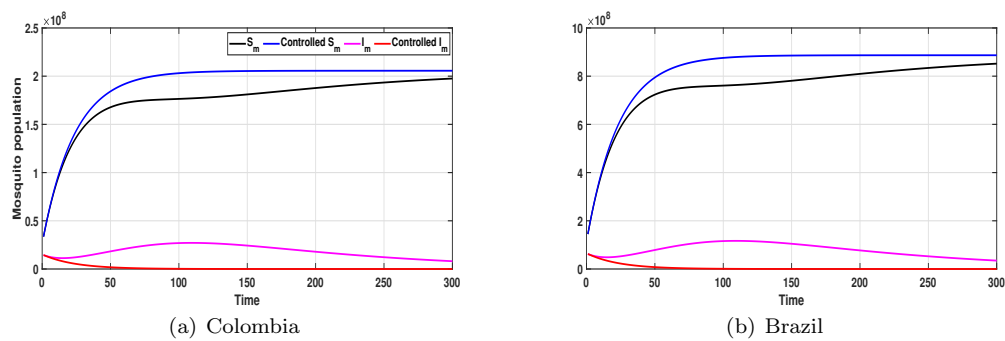


Fig. 5.6: Simulations of the mosquito population in Colombia and Brazil with the activation of different controls.

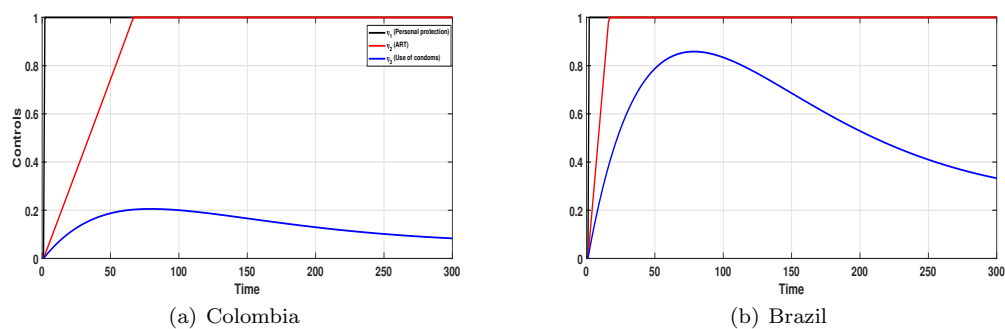


Fig. 5.7: Simulations of the behaviour of the controls in Colombia and Brazil.

Compartments  $I_z$  and  $A$  are controlled to a smaller size than the  $\eta_1 = \eta_2 = \eta_3 = 0$  simulation, while compartments  $I_h$  and  $I_{hz}$  have a larger size owing to the ART that prevents infected people from reaching the AIDS stage. However, the mixed strategies were maintained at their approximate total capacities, as illustrated in Figure 5.8.

In addition, the size of the infected mosquito population remained below the initial condition which prevented the spread of ZIKV due to the effect of the  $\eta_1$  control.

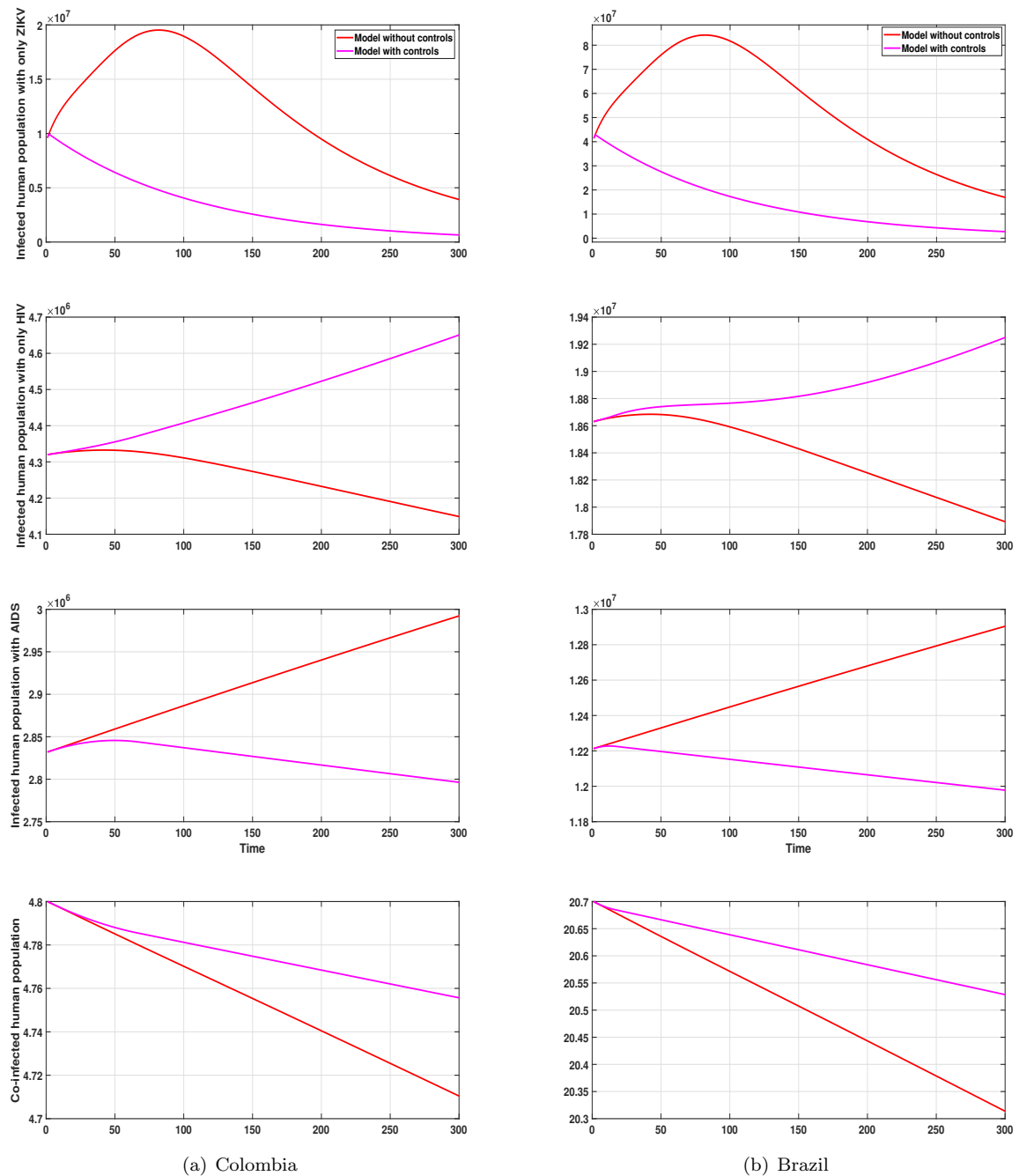


Fig. 5.8: Simulations of controlling infected human sizes in Colombia and Brazil.

Finally, to corroborate the behaviour of the co-infected human and the mosquitoes populations with respect to the variation of the combined controls  $\eta_1$ ,  $\eta_2$  and  $\eta_3$ , (see Figures 5.9 and 5.10), we have performed some additional numerical experiments. Figure 5.9 shows that the concurrent activation of  $\eta_1$  (personal protection) and  $\eta_2$  (ART) generate comparable trends in the co-infected individuals with zika and HIV within the contexts of Colombia and Brazil. Hence, in Figures 5.9 (a)-(b), we investigated the co-infection patterns by fixing the control  $\eta_1$  for personal protection and increasing gradually the ART control from 0 to its maximum value 1 with an increment value of  $\Delta\eta_1 = \Delta\eta_2 = 0.003$ . In both cases for Brazil and Colombia, the increase of the personal protection did not play a significant role as the gradual increase of ART for the co-infection. However, the personal protection plays an important role to reduce the overall ZIKV infected population. Analogously, the simultaneous implementation of ART and condoms use ( $\eta_3$ ) in Colombian and Brazil reduce the number of co-infected individuals burden. Hence, in Figures 5.9 (c-d), the condom use plays a more significant role in reducing the size of co-infected size.

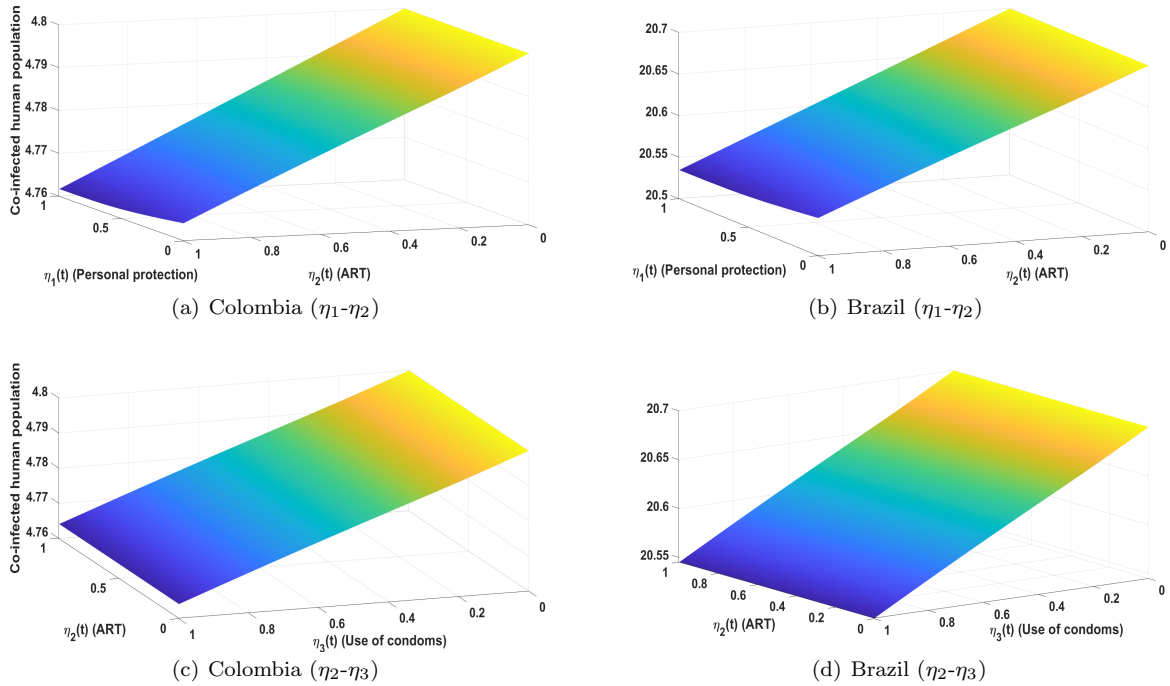


Fig. 5.9: Simulation of the effects of combined  $\eta_1$ - $\eta_2$  and  $\eta_2$ - $\eta_3$  on the co-infected human population in Colombia and Brazil.

This supports the outcomes derived from the simulations presented in Figure 5.8, wherein the control strategy involving the simultaneous application of all controls above was previously established. The dynamics exhibited by the population of zika virus-carrying mosquitoes, when subjected to concurrent interventions involving personal protection, ART, and condom use, diverge from those observed within the co-infected human population. This contrast is evident upon examining Figure 5.10, wherein distinct patterns manifest for Colombia and Brazil. Notably, the impact of personal protection emerges as more pronounced than that of ART, as underscored by the observation that mosquito density exhibits heightened levels when the efficacy of personal protection approaches to zero. The limited influence of sexual transmission dynamics of zika and HIV on mosquito density substantiates this outcome. Conversely, upon simultaneous implementation of ART and condom use in Colombia and Brazil, the peaks in mosquito densities materialize when both controls are administered at 50%. In contrast, the lowest densities align with situations with no controls or controls implemented at 100%. These observations significantly explain the complex interplay between control strategies and their varying effects on human and mosquito populations in the HIV/ZIKV co-infection context. This

information could guide policymakers and public health authorities in making informed decisions regarding the most effective strategies for managing and controlling these diseases.

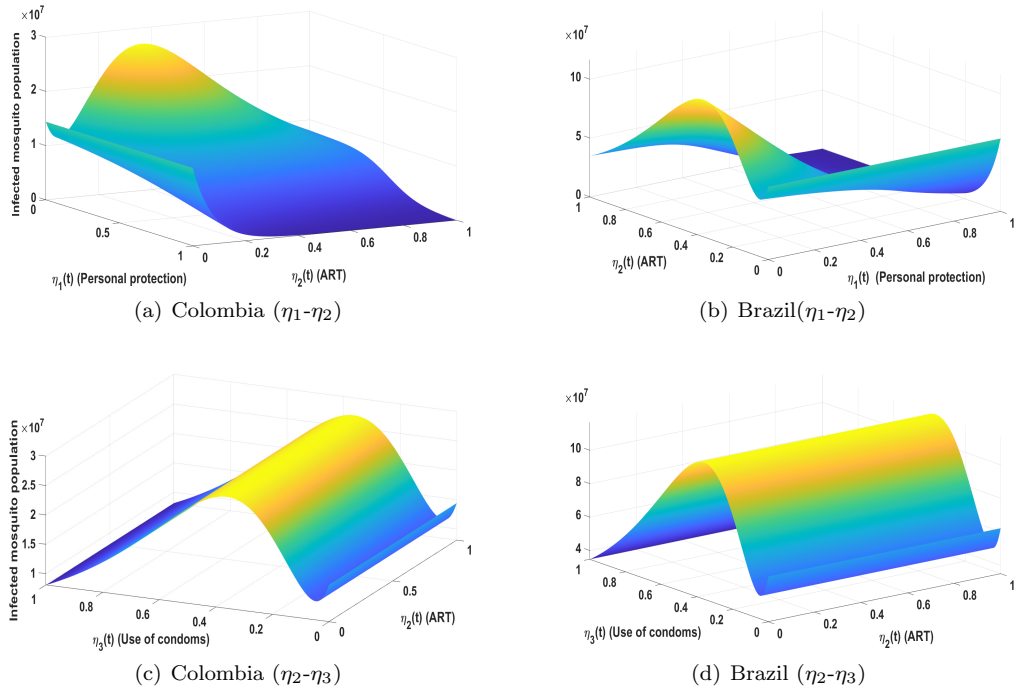


Fig. 5.10: Simulation of the effects of combined  $\eta_1$ - $\eta_2$  and  $\eta_2$ - $\eta_3$  on the infected mosquito population in Colombia and Brazil.

## 6 Discussion and concluding remarks

The first reported cases of HIV/ZIKV co-infection in Colombia and Brazil highlighted the potential interactions between these two viruses. The co-circulation of these infections in South America presented a unique challenge for public health officials, as both viruses were known to be transmitted through sexual contact and had overlapping clinical symptoms.

The mathematical modelling conducted in this study was used to consider the transmission dynamics of both viruses in co-infected individuals, allowing for the evaluation of different intervention scenarios. The findings of this study were particularly relevant during the 2015-2016 zika outbreak in South America, which overlapped with the ongoing HIV epidemic in the region. By identifying the patterns of co-infection and their potential impact on transmission, the results of this study could inform public health strategies to control and prevent the spread of both viruses.

On the one hand, numerical simulations conducted with parameter values for Colombia provided valuable insights into the potential impact of HIV/ZIKV co-infection. By comparing three distinct scenarios about co-infection probabilities (high, medium, and low), the study demonstrated that an increase in these parameters led to a higher density of co-infected individuals. By comparing the qualitative behaviour of zika and HIV in Brazil and Colombia, we found the following results: First, both countries exhibited similar trends in spreading and stabilizing these viruses, with differences primarily attributable to population density. Second, individuals infected with ZIKV demonstrated greater variability in their behaviour than those infected with HIV/AIDS. This suggests that ZIKV infection displayed a diverse and fluctuating progression with various manifestations, potentially influenced by multiple factors. In contrast, individuals infected with HIV/AIDS exhibited more consistent and stable behaviour over time. Third, the simulation results demonstrated that

increasing the values of the co-infection probabilities  $\omega_1$  and  $\omega_2$  could lead to a higher population density of co-infected individuals. This finding underscores the importance of implementing effective strategies to prevent and control the spread of these viruses, particularly in pregnant women, to prevent congenital complications.

The primary preventative methods for zika and HIV infection included avoiding mosquito bites, using condoms during sexual activity, and a treatment strategy such as antiretroviral therapy (ART). Given that zika is mainly spread by mosquitoes, we established a timely control to describe measures such as using insect repellent, donning long sleeves, and staying indoors during prime mosquito-biting hours are all personal protection measures. In addition, we illustrated a control for condoms use to lower the risk of transmission of zika, which can also spread sexually. Similarly, since sexual contact is the primary way HIV spreads, the most effective strategy to prevent HIV transmission during sex is to use condoms appropriately and regularly. Additionally, we incorporated a control variable for ART, which included using a variety of HIV medications to successfully suppress the virus, maintain or enhance immune function, and lower the risk of transmission.

In summary, this study highlighted the need for continued research on the transmission dynamics of zika and HIV/AIDS and developing effective intervention strategies to control and prevent their spread. Future work in this field plans to incorporate compartments of women giving birth to babies with and without congenital malformations to understand the impact of co-infection in children better. Including these compartments would allow for a more detailed assessment of the long-term effects of co-infection on child health outcomes, including the potential for developmental delays, neurological deficits, and other complications. This approach could also facilitate the development of more targeted prevention and treatment strategies for the affected children and their families. Ultimately, this research is critical for improving our understanding of the complex interactions between HIV and zika and developing effective public health interventions to mitigate their impact on affected individuals and communities.

## Acknowledgements

The authors appreciate the support provided by the One Health Modelling Network for Emerging Infections (OMNI-RÉUNIS) and Mathematics for Public Health (MfPH), which are financially supported by the Natural Sciences and Engineering Research Council of Canada (NSERC) and the Public Health Agency of Canada (PHAC).

## References

1. W. E. Villamil-Gómez, Álvaro Rosendo Sánchez-Herrera, H. Hernández-Prado, J. Hernández-Iriarte, K. Díaz-Ricardo, O. Vergara-Serpa, J. Castellanos, J. E. Portela-Gaviria, S. Patiño-Valencia, D. C. Vargas-Bedoya, A. F. Orozco-Villa, S. S. Reyes-Guerrero, J. D. Castrillón-Spitia, D. R. Murillo-García, V. Henao-SanMartin, J. J. Londoño, H. Bedoya-Rendón, J. de Jesús Cárdenas-Pérez, J. A. Cardona-Ospina, G. J. Lagos-Grisales, and A. J. Rodríguez-Morales, "Zika virus and HIV co-infection in five patients from two areas of Colombia," 2018.
2. V. M. Cao-Lormeau, A. Blake, S. Mons, S. Lastère, C. Roche, J. Vanhomwegen, T. Dub, L. Baudouin, A. Teissier, P. Larre, A. L. Vial, C. Decam, V. Choumet, S. K. Halstead, H. J. Willison, L. Musset, J. C. Manuguerra, P. Despres, E. Fournier, H. P. Mallet, D. Musso, A. Fontanet, J. Neil, and F. Ghawché, "Guillain-Barré syndrome outbreak associated with Zika virus infection in French Polynesia: a case-control study," *The Lancet*, vol. 387, 2016.
3. E. Oehler, L. Watrin, P. Larre, I. Leparc-Goffart, S. Lastère, F. Valour, L. Baudouin, H. P. Mallet, D. Musso, and F. Ghawche, "Zika virus infection complicated by Guillain-Barré syndrome—case report, French Polynesia, December 2013," *Eurosurveillance*, vol. 19, 2014.
4. D. W. Smith and J. Mackenzie, "Zika virus and Guillain-Barré syndrome: another viral cause to add to the list," 2016.
5. J. Mlakar, M. Korva, N. Tul, M. Popović, M. Poljšak-Prijatelj, J. Mraz, M. Kolenc, K. R. Rus, T. V. Vipotnik, V. F. Vodusek, A. Vizjak, J. Pizem, M. Petrovec, and T. A. Županc, "Zika virus associated with microcephaly," *New England Journal of Medicine*, vol. 374, 2016.
6. G. Calvet, R. S. Aguiar, A. S. Melo, S. A. Sampaio, I. De Filippis, A. Fabri, E. S. Araujo, P. C. de Sequeira, M. C. de Mendonça, L. de Oliveira, *et al.*, "Detection and sequencing of Zika virus from amniotic fluid of fetuses with microcephaly in Brazil: a case study," *The Lancet Infectious Diseases*, vol. 16, no. 6, pp. 653–660, 2016.
7. A. F. Kabapy, H. Z. Shatat, and E. W. A. El-Wahab, "Attributes of HIV infection over decades (1982–2018): A systematic review and meta-analysis," 2020.
8. J. C. Tilton and R. W. Doms, "Entry inhibitors in the treatment of HIV-1 infection," 2010.
9. B. Atkinson, P. Hearn, B. Afrough, S. Lumley, D. Carter, E. J. Aarons, A. J. Simpson, T. J. Brooks, and R. Hewson, "Detection of Zika virus in semen," 2016.

10. A. C. Gourinat, O. O'Connor, E. Calvez, C. Goarant, and M. Dupont-Rouzeyrol, "Detection of Zika virus in urine," *Emerging Infectious Diseases*, vol. 21, 2015.
11. D. Musso, C. Roche, E. Robin, T. Nhan, A. Teissier, and V.-M. Cao-Lormeau, "Potential sexual transmission of Zika virus," *Emerging infectious diseases*, vol. 21, no. 2, p. 359, 2015.
12. H. A. Rothan, M. R. Bidokhti, and S. N. Byrareddy, "Current concerns and perspectives on zika virus co-infection with arboviruses and HIV," *Journal of autoimmunity*, vol. 89, pp. 11–20, 2018.
13. K. E. Sherman, S. D. Rouster, L. X. Kong, T. M. Shata, T. Archampong, A. Kwara, M. T. Aliota, and J. T. Blackard, "Zika virus exposure in an HIV-infected cohort in Ghana," 2018.
14. E. C. João, O. da C. Ferreira, M. I. Gouvêa, M. de Lourdes B. Teixeira, A. Tanuri, L. M. Higa, D. A. Costa, R. Mohana-Borges, M. B. Arruda, H. J. Matos, M. L. Cruz, W. Mendes-Silva, and J. S. Read, "Pregnant women co-infected with HIV and Zika: Outcomes and birth defects in infants according to maternal symptomatology," *PLoS ONE*, vol. 13, 2018.
15. C. D. Zorrilla, A. M. Mosquera, S. Rabionet, and J. Rivera-Viñas, "HIV and Zika in pregnancy: parallel stories and new challenges," *Obstetrics & Gynecology International Journal*, vol. 5, no. 6, 2016.
16. P. Brasil, J. P. Pereira, M. E. Moreira, R. M. R. Nogueira, L. Damasceno, M. Wakimoto, R. S. Rabello, S. G. Valderramos, U.-A. Halai, T. S. Salles, A. A. Zin, D. Horovitz, P. Daltro, M. Boechat, C. R. Gabaglia, P. C. de Sequeira, J. H. Pilotto, R. Medialdea-Carrera, D. C. da Cunha, L. M. A. de Carvalho, M. Pone, A. M. Siqueira, G. A. Calvet, A. E. R. Baião, E. S. Neves, P. R. N. de Carvalho, R. H. Hasue, P. B. Marschik, C. Einspieler, C. Janzen, J. D. Cherry, A. M. B. de Filippis, and K. Nielsen-Saines, "Zika virus infection in pregnant women in Rio de Janeiro," *New England Journal of Medicine*, vol. 375, 2016.
17. A. Aschengrau, M. M. Mussi-Pinhata, J. Moye, N. Chakhtoura, K. Patel, P. L. Williams, B. Karalius, P. A. Garvie, D. Monte, F. Whalen, J. Lebov, and G. R. Seage, "An international prospective cohort study of HIV and Zika in infants and pregnancy (HIV-ZIP): Study protocol," *Frontiers in Global Women's Health*, vol. 2, 2021.
18. J. P. Romero-Leiton, J. E. Castellanos, and E. Ibargüen-Mondragón, "An optimal control problem and cost-effectiveness analysis of malaria disease with vertical transmission applied to San Andrés de Tumaco (Colombia)," *Computational and Applied Mathematics*, vol. 38, 2019.
19. P. V. D. Driessche and J. Watmough, "Reproduction numbers and sub-threshold endemic equilibria for compartmental models of disease transmission," *Mathematical Biosciences*, vol. 180, 2002.
20. S. Bañuelos, M. Martínez, C. Mitchell, and A. Prieto-Langarica, "Using mathematical modelling to investigate the effect of the sexual behaviour of individuals and vector control measures on Zika," *Letters in Biomathematics*, vol. 6, no. 1, pp. 1–19, 2019.
21. N. Chitnis, J. M. Hyman, and J. M. Cushing, "Determining important parameters in the spread of malaria through the sensitivity analysis of a mathematical model," *Bulletin of Mathematical Biology*, vol. 70, 2008.
22. L. S. Pontryagin, V. Boltyanskii, R. Gamkrelidze, E. Mishchenko, K. Trirogoff, and L. Neustadt, *LS Pontryagin Selected Works: The Mathematical Theory of Optimal Processes*. Routledge, 2018.
23. B. Joob and V. Wiwanitkit, "Concurrent HIV and Zika virus infection, a problem to be address in HIV medicine," *Int J Virol AIDS*, vol. 3, p. 035, 2017.
24. M. R. Bidokhti, D. Dutta, L. S. Madduri, S. M. Woollard, R. Norgren, L. Giavedoni, and S. N. Byrareddy, "SIV/SHIV-Zika co-infection does not alter disease pathogenesis in adult non-pregnant rhesus macaque model," *PLoS Neglected Tropical Diseases*, vol. 12, 2018.
25. K. Prieto and J. P. Romero-Leiton, "Current forecast of HIV/AIDS using Bayesian inference," *Natural Resource Modeling*, vol. 34, 2021.
26. D. Gao, Y. Lou, D. He, T. C. Porco, Y. Kuang, G. Chowell, and S. Ruan, "Prevention and control of zika as a mosquito-borne and sexually transmitted disease: a mathematical modeling analysis," *Springer*, 2016.
27. S. K. Biswas, U. Ghosh, and S. Sarkar, "Mathematical model of Zika virus dynamics with vector control and sensitivity analysis," *Infectious Disease Modelling*, vol. 5, pp. 23–41, 2020.
28. W. H. Organization *et al.*, "Zika strategic response plan quarterly update," tech. rep., World Health Organization, 2016.
29. L. J. Forero-Martínez, R. Murad, M. Calderón-Jaramillo, and J. C. Rivillas-García, "Zika and women's sexual and reproductive health: Critical first steps to understand the role of gender in the colombian epidemic," *International Journal of Gynecology and Obstetrics*, vol. 148, 2020.
30. C. Prachniak-Rincón and J. V. D. Onís, "HIV and the right to health in Colombia," *Health and Human Rights*, vol. 18, 2016.
31. D. Bancroft, G. M. Power, R. T. Jones, E. Massad, J. B. Iriat, R. Preet, J. Kinsman, and J. G. Logan, "Vector control strategies in Brazil: A qualitative investigation into community knowledge, attitudes and perceptions following the 2015-2016 Zika virus epidemic," *BMJ Open*, vol. 12, 2022.
32. A. S. Benzaken, G. F. Pereira, L. Costa, A. Tanuri, A. F. Santos, and M. A. Soares, "Antiretroviral treatment, government policy and economy of HIV/AIDS in Brazil: Is it time for HIV cure in the country?," 2019.
33. J. Hainzl, M. D. Leko, A. Pignedoli, and B. Vrdoljak, *12: Ordinary Differential Equations and Dynamical Systems*. 2022.
34. C. Castillo-Chavez and H. R. Thieme, "Asymptotically autonomous epidemic models," *Science*, vol. 94, 1994.
35. C. C. McCluskey and J. S. Muldowney, "Bendixson-Dulac criteria for difference equations," *Journal of Dynamics and Differential Equations*, vol. 10, 1998.
36. E. Roxin and D. L. Lukes, "Differential equations: Classical to controlled.," *The American Mathematical Monthly*, vol. 92, 1985.

## A Appendices

### A.1 Proof that $\mathbf{E}_{h_0}$ is GAS when $\mathcal{R}_h < 1$

Let  $\mathbf{X}$  be the vector field given by the right side hand of System (A.2). It is enough to prove the existence of a Lyapunov function for the translated system

$$\dot{\mathbf{X}} = F(\mathbf{X} + \mathbf{E}_{h_0}) - F(\mathbf{E}_{h_0}) = f(\mathbf{X}),$$

where the system  $\dot{\mathbf{Y}} = F(\mathbf{Y})$  has  $\mathbf{Y} = 0$  as equilibrium solution. Let us consider the function

$$V^*(S, I_h, A) = \frac{1}{\sigma_1 + \mu} I_h,$$

and define

$$V(\bar{S}, \bar{I}_h, \bar{A}) = V^* \left( S - \frac{A}{\mu}, I_h, A \right). \quad (\text{A.1})$$

We verify that the function  $V$  defined on (A.1) is a Lyapunov function. Indeed,  $V$  is positive definite, that is,  $V(\mathbf{E}_{h_0}) = V^*(\mathbf{0}) = 0$  and  $V > 0$  for all  $(\bar{S}, \bar{I}_h, \bar{A}) \neq \mathbf{E}_{h_0}$  in  $\Omega_h$ . Additionally, the orbital derivative of  $V$  along the trajectories of system (2.2) is

$$\begin{aligned} \dot{V} &= \frac{\partial V^*}{\partial \left( S - \frac{A}{\mu} \right)} \dot{S} + \frac{\partial V^*}{\partial I_h} \dot{I}_h + \frac{\partial V^*}{\partial A} \dot{A} \\ &= \frac{1}{\sigma_1 + \mu} (\beta_h I_h S - (\sigma_1 + \mu) I_h) \\ &\leq \frac{1}{\sigma_1 + \mu} (\sigma_1 + \mu) \left( \frac{\beta_h A}{\sigma_1 + \mu} - 1 \right) I_h \\ &= (\mathcal{R}_h - 1) I_h \leq 0, \quad \forall I_h \geq 0. \end{aligned}$$

Let  $\Delta = \{(S, I_h, A) \in \mathbb{R}_+^3 : \dot{V} = 0\} \subset \{(S, I_h, A) \in \mathbb{R}_+^3 : I_h = 0\}$  and  $\Delta' \subset \Delta$  the largest invariant set respect to (2.2). It can be easily showed that  $\Delta' = \{\mathbf{E}_{h_0}\}$ . Therefore by the LaSalle's invariance principle [33],  $\mathbf{E}_{h_0}$  is a global attractor whenever  $\mathcal{R}_h < 1$ .

### A.2 Proof that $\mathbf{E}_h^*$ is GAS when $\mathcal{R}_h > 1$

Note that the third equation of System (2.2) is uncoupled in the variable  $S$  and its equilibrium is  $I_h = \frac{\mu_h + \mu}{\sigma_1} A$ . Replacing this value in the two first equations, we obtain the planar system

$$\begin{cases} \frac{dS}{dt} = \Lambda - \beta_h \frac{\mu_h + \mu}{\sigma_1} SA - \mu S \\ \frac{dA}{dt} = \beta_h AS - (\sigma_1 + \mu) A. \end{cases} \quad (\text{A.2})$$

Therefore, solutions to system (2.2) tend asymptotically to those of the planar system (A.2) (see e.g. [34]). The Dulac criterion [35] claims that if there exists a real continuously differentiable function  $\phi(S, A)$  such that  $\nabla \cdot [\phi(S, A)\mathbf{X}(S, A)] \neq 0$ , where  $\mathbf{X}(S, A) = (F(S, A), G(S, A))$  is the right side hand of system (A.2), then there are no periodic orbits contained entirely inside  $\Omega_h$ . Let

$$\phi(S, A) = \frac{1}{SA} \quad \text{for } S > 0, A > 0,$$

then

$$\begin{aligned} \nabla \cdot [\phi(S, A)\mathbf{X}(S, A)] &= \frac{\partial(F\phi)}{\partial S} + \frac{\partial(G\phi)}{\partial A} \\ &= \frac{\partial}{\partial S} \left( \frac{\Lambda}{SA} - \frac{\beta_h(\mu_h + \mu)}{\sigma_1 SA} SA - \frac{\mu S}{SA} \right) + \frac{\partial}{\partial A} \left( \frac{\beta_h AS}{SA} - \frac{\sigma_1 + \mu}{SA} A \right) \\ &= \frac{\partial}{\partial S} \left( \frac{\Lambda}{SA} - \frac{\beta_h(\mu_h + \mu)}{\sigma_1} - \frac{\mu}{A} \right) + \frac{\partial}{\partial A} \left( \beta_h - \frac{\sigma_1 + \mu}{S} \right) \\ &= -\frac{\Lambda}{AS^2} < 0, \quad \text{for } S, A > 0. \end{aligned}$$

Thus, there are no periodic orbits in  $\Omega_h$ . Given that  $\Omega_h$  is positively invariant, and the endemic equilibrium exists if  $\mathcal{R}_h > 1$ , it follows from the Poincaré-Bendixson Theorem [35] that all solutions of the system starting in  $\Omega_h$  remain in  $\Omega_h$  for all  $t$ . Thus, because of the absence of periodic orbits in  $\Omega_h$ , this implies that the unique endemic equilibrium of System (2.2) is GAS when  $\mathcal{R}_h > 1$ .

### A.3 Proof of Lemma 1

We prove item *i*); all others are proved in a similar way. On the one hand, from the definition of  $\mathcal{R}_z^*$ , we immediately have that if  $\mathcal{R}_z^* = 2\mathcal{R}_{z_1} + \bar{\mathcal{R}}_{z_2} < 1$ , then  $2\mathcal{R}_{z_1} < 1$ . On the other hand,

$$\begin{aligned} \mathcal{R}_z^* < 1 &\Rightarrow \mathcal{R}_z^2 + 2\mathcal{R}_{z_1}(1 - \mathcal{R}_z) < 1 \\ &\Rightarrow \mathcal{R}_z(1 - 2\mathcal{R}_{z_1}) + 2\mathcal{R}_z \\ &\Rightarrow \mathcal{R}_z(1 - 2\mathcal{R}_{z_1}) < 1 - 2\mathcal{R}_z, \quad (2\mathcal{R}_{z_1} < 1) \\ &\Rightarrow \mathcal{R}_z < 1. \end{aligned}$$

### A.4 Proof of the condition $R^* < R_{max}$

We have to prove that  $R^* < R_{max}$  is satisfied. To this end, we consider the polynomial  $p(R)$  associated to system (2.20), whose coefficients are in equation (2.21). The graph of  $p(R)$  is a parabola that opens upward (see Figure A.1). Since  $R^* > 0$  and  $p(0) = c < 0$  as long as  $\mathcal{R}_{z_1} + \mathcal{R}_{z_2} > 1$ , then to ensure that  $R^* < R_{max}$ , it is enough to prove that  $p(R_{max}) > 0$ . In fact

$$\begin{aligned} p(R_{max}) &= aR_{max}^2 + bR_{max} + c \\ &= \frac{\beta_z \Lambda \alpha_m \mu}{\delta_z R_{max}} R_{max}^2 + \left[ \left( \frac{\beta_m \alpha_m \Lambda m}{\mu_m} + \beta_z \mu_m \right) \frac{\Lambda}{R_{max}} + [\alpha_m \mu (\mu_z + \delta_z + \mu) - \beta_z \Lambda \alpha_m] \frac{\mu}{\delta_z} \right] R_{max} \\ &\quad + (\mu_z + \delta_z + \mu) \mu \mu_m (1 - \mathcal{R}_z^*) \\ &= \frac{\beta_z \Lambda \alpha_m \mu}{\delta_z} R_{max} + \left( \frac{\beta_m \alpha_m \Lambda m}{\mu_m} + \beta_z \mu_m \right) \Lambda + [\alpha_m \mu (\mu_z + \delta_z + \mu) - \beta_z \Lambda \alpha_m] \frac{\mu}{\delta_z} R_{max} \\ &\quad + (\mu_z + \delta_z + \mu) \mu \mu_m (1 - \mathcal{R}_z^*) \\ &= \left( \frac{\beta_m \alpha_m \Lambda m}{\mu_m} + \beta_z \mu_m \right) \Lambda + \frac{\alpha_m \mu^2 (\mu_z + \delta_z + \mu) R_{max}}{\delta_z} + (\mu_z + \delta_z + \mu) \mu \mu_m (1 - \mathcal{R}_z^*) \\ &= (\mu_z + \delta_z + \mu) \mu \mu_m (\mathcal{R}_z^* (\mathcal{R}_z^* - \mathcal{R}_z) + \alpha_m \Lambda \mu^2 + (\mu_z + \delta_z + \mu) \mu \mu_m) \\ &= \alpha_m \Lambda \mu^2 + (\mu_z + \delta_z + \mu) \mu \mu_m > 0. \end{aligned}$$

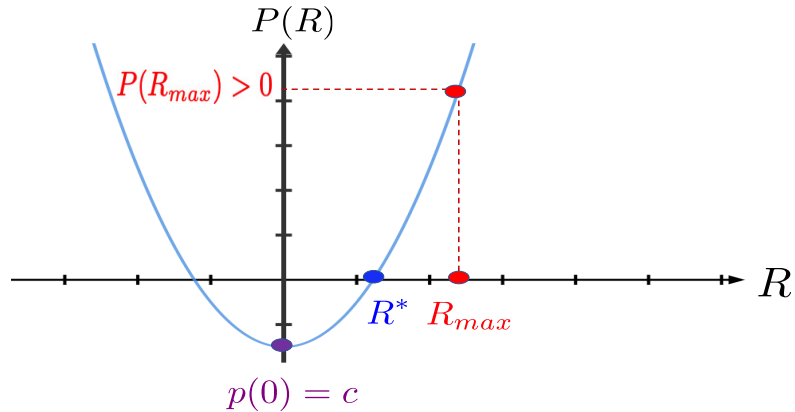


Fig. A.1: Polynomial  $p(R)$  associated to system (2.20).

### A.5 Proof that $\mathbf{E}_{z_0}$ is GAS when $\mathcal{R}_z^* < 1$

We will use  $\kappa = \mu_z + \delta_z + \mu$  and the notation and reasoning analogous to that used in the proof of Proposition ??, with functions

$$V^*(S, I_z, R, S_m, I_m) = \left( S - \frac{\Lambda}{\mu} \log \frac{S\mu}{\Lambda} \right) + I_z + \frac{\beta_m \Lambda}{\mu \mu_m} \left( S_m - \frac{\Lambda_m}{\mu_m} \log \frac{S_m \mu_m}{\Lambda_m} \right) + \frac{\beta_m \Lambda}{\mu \mu_m} I_m$$

and

$$V(\bar{S}, \bar{I}_z, \bar{R}, \bar{S}_m, \bar{I}_m) = V^* \left( S - \frac{\Lambda}{\mu}, I_z, R, S_m, I_m - \frac{\Lambda_m}{\mu_m} \right). \quad (\text{A.3})$$

We must prove that  $V$  defined in (A.3) is a Lyapunov function.  $V$  is positive definite and the orbital derivative of  $V$  along the trajectories of (2.9) is

$$\begin{aligned} \dot{V} &= \left( 1 - \frac{\Lambda}{\mu S} \right) \dot{S} + \dot{I}_z + \frac{\beta_m \Lambda}{\mu \mu_m} \left( 1 - \frac{\Lambda_m}{\mu_m S_m} \right) \dot{S}_m + \frac{\beta_m \Lambda}{\mu \mu_m} \dot{I}_m \\ &= \left( 1 - \frac{\Lambda}{\mu S} \right) (\Lambda - \beta_m I_m S - \beta_z I_z S - \mu S) + (\beta_m I_m S + \beta_z I_z S - \kappa I_z) \\ &\quad + \frac{\beta_m \Lambda}{\mu \mu_m} \left( 1 - \frac{\Lambda_m}{\mu_m S_m} \right) (\Lambda_m - \alpha_m I_z S_m - \mu_m S_m) + \frac{\beta_m \Lambda}{\mu \mu_m} (\alpha_m I_z S_m - \mu_m I_m) \\ &= (\Lambda - \mu S) - \frac{\Lambda}{\mu S} (\Lambda - \mu S) + \frac{\Lambda}{\mu S} (\beta_m I_m + \beta_z I_z) S - \kappa I_z + \frac{\beta_m \Lambda}{\mu \mu_m} (\Lambda_m - \mu_m S_m) \\ &\quad - \frac{\beta_m \Lambda \Lambda_m}{\mu \mu_m S_m \mu_m} (\Lambda_m - \mu_m S_m) + \frac{\beta_m \Lambda \Lambda_m \alpha_m S_m I_z}{\mu \mu_m S_m \mu_m} - \frac{\beta_m \Lambda \mu_m I_m}{\mu \mu_m} \\ &= -\frac{(\Lambda - \mu S)^2}{\mu S} - \frac{\beta_m \Lambda}{\mu \mu_m^2} \frac{(\Lambda_m - \mu_m S_m)^2}{S_m} + \left( \frac{\Lambda}{\mu} \beta_z + \frac{\beta_m \alpha_m \Lambda_m \Lambda}{\mu \mu_m^2} - \kappa \right) I_z \\ &= -\frac{(\Lambda - \mu S)^2}{\mu S} - \frac{\beta_m \Lambda}{\mu \mu_m^2} \frac{(\Lambda_m - \mu_m S_m)^2}{S_m} + \kappa (\mathcal{R}_z^* - 1) I_z. \end{aligned}$$

Note that the last expression in the above inequality is negative if  $\mathcal{R}_z^* < 1$  and for  $S = \frac{\Lambda}{\mu}$ ,  $S_m = \frac{\Lambda_m}{\mu_m}$  and  $I_z = I_m = 0$ . Finally, using the LaSalle's invariance principle [33],  $\mathbf{E}_{z_0}$  defined in (2.11) is a global attractor whenever  $\mathcal{R}_z^* < 1$ .

### A.6 Sensitivity index of $\mathcal{R}_z$ with respect to $\beta_z$

We have

$$\begin{aligned} \frac{\partial \mathcal{R}_z}{\partial \beta_z} &= \frac{\partial}{\partial \beta_z} \left( \frac{\beta_z \Lambda}{2\mu \kappa_1} + \sqrt{\left( \frac{\beta_z \Lambda}{2\mu \kappa_1} \right)^2 + \frac{\alpha_m \beta_m \Lambda_m \Lambda}{\mu \mu_m^2 \kappa_1}} \right) \\ &= \frac{\Lambda}{2\mu(\delta_z + \mu + \mu_z)} + \frac{\beta_z \Lambda^2}{4\mu^2(\delta_z + \mu + \mu_z)^2 \sqrt{\frac{\beta_z^2 \Lambda^2}{4\mu^2(\delta_z + \mu + \mu_z)^2} + \frac{\alpha_m \beta_m \Lambda_m \Lambda}{\mu \mu_m^2(\delta_z + \mu + \mu_z)}}}. \end{aligned}$$

Then, it is enough to compute the expression for

$$\frac{\partial \mathcal{R}_z}{\partial \beta_z} \frac{\beta_z}{\mathcal{R}_z} = \frac{\partial \mathcal{R}_z}{\partial \beta_z} \frac{\beta_z}{\frac{\beta_z \Lambda}{2\mu \kappa_1} + \sqrt{\left( \frac{\beta_z \Lambda}{2\mu \kappa_1} \right)^2 + \frac{\alpha_m \beta_m \Lambda_m \Lambda}{\mu \mu_m^2 \kappa_1}}}.$$

### A.7 Proof of Proposition 7

All state variables and controls are non-negative and, for  $i = \{1, 2, 3\}$ , the set of control variables  $\eta_i \in \mathcal{A}$  is also convex and closed. We note that the boundedness of the optimal system (4.1) determines the compactness for the existence of the optimal control. Moreover, there exists a constant  $\nu > 1$ ,  $\omega_1 = \min(d_1, d_2, d_3)$ , and  $\omega_2 > 0$  such that

$$\mathcal{J}(\eta) \geq \omega_1 \|\eta\|^\nu - \omega_2. \quad (\text{A.4})$$

Therefore, according to [36], the controlled system (4.1) admits an optimal control solution  $\eta^*$ .

## A.8 Proof of Proposition 8

We have

$$\begin{aligned}
\frac{p_1}{dt} &= -\frac{\partial H}{\partial S} = p_1 [(1 - \eta_1)\beta_m I_m + (1 - \eta_3)(\beta_z I_z + \beta_h I_h) + \mu] - p_2 [(1 - \eta_1)\beta_m I_m + (1 - \eta_3)\beta_z I_z] \\
&\quad - p_3 [(1 - \eta_3)\beta_h I_h], \\
\frac{p_2}{dt} &= -\frac{\partial H}{\partial I_z} = -c_1 + p_1(1 - \eta_3)\beta_z S - p_2 [(1 - \eta_3)\beta_z S - \omega_2(1 - \eta_3)\beta_h I_h - (\mu_z + \delta_z + \mu)] - p_3(1 - \eta_3)\beta_z I_h \\
&\quad - p_6 \delta_z + p_7(1 - \eta_1)\alpha_m S_m - p_8(1 - \eta_1)\alpha_m S_m, \\
\frac{p_3}{dt} &= -\frac{\partial H}{\partial I_h} = -c_2 + p_1(1 - \eta_3)\beta_h S + p_2 \omega_2(1 - \eta_3)\beta_h I_z - p_3 [\omega_1 [(1 - \eta_1)\beta_m I_m + (1 - \eta_3)\beta_z I_z] \\
&\quad - (1 - \eta_2)\sigma_1 - \mu] - p_4 [\omega_1 [(1 - \eta_1)\beta_m I_m + (1 - \eta_3)\beta_z I_z] + \omega_2(1 - \eta_3)\beta_h I_z] \\
&\quad - p_5(1 - \eta_2)\sigma_1, \\
\frac{p_4}{dt} &= -\frac{\partial H}{\partial I_{hz}} = -c_3 + p_4(\epsilon \delta_z + (1 - \eta_2)\sigma_2 + \mu_{hz} + \mu) - p_5(1 - \eta_2)\sigma_2 - p_6 \epsilon \delta_z + p_7(1 - \eta_1)\alpha_m S_m \\
&\quad - p_8(1 - \eta_1)\alpha_m S_m, \\
\frac{p_5}{dt} &= -\frac{\partial H}{\partial A} = -c_5 + p_5(\mu_h + \mu), \\
\frac{p_6}{dt} &= -\frac{\partial H}{\partial R} = p_6 \mu, \\
\frac{p_7}{dt} &= -\frac{\partial H}{\partial S_m} = p_7((1 - \eta_1)\alpha_m(I_z + I_{hz}) + \mu_m) - p_8(1 - \eta_1)\alpha_m(I_z + I_{hz}), \\
\frac{p_8}{dt} &= -\frac{\partial H}{\partial I_m} = -c_4 + p_1(1 - \eta_1)\beta_m S - p_2(1 - \eta_1)\beta_m S + p_3(1 - \eta_1)\beta_m I_h - p_4 \omega_1(1 - \eta_1)\beta_m I_h + p_8 \mu_m,
\end{aligned}$$

with transversality conditions  $p_i(T) = 0$ , for  $i = \{1, 2, 3, 4, 5, 6, 7, 8\}$ . According to PMP, the optimal conditions are

$$\begin{aligned}
\frac{\partial H}{\partial \eta_1} &= d_1 \eta_1 - ((p_2 - p_1)S + (p_4 - p_3)I_h) \beta_m I_m - (p_8 - p_7)\alpha_m(I_z + I_{hz})S_m = 0, \\
\frac{\partial H}{\partial \eta_2} &= d_2 \eta_2 - (p_5 - p_3)\sigma_1 I_h - (p_5 - p_4)\sigma_2 I_{hz} = 0, \\
\frac{\partial H}{\partial \eta_3} &= d_3 \eta_3 - (p_2 - p_1)\beta_z I_z S - (p_3 - p_1)\beta_h I_h S - (p_4 - p_3)\omega_1 \beta_z I_z I_h - (p_4 - p_2)\omega_2 \beta_h I_z I_h = 0.
\end{aligned}$$

Hence, we get assertions (8). This completes the proof.